The physiological determinant of the storage of memory trace identity

A dissertation submitted to the

Graduate School of Innovative Life Sciences

University of Toyama, Japan

For the degree of

Doctor of Philosophy (Medicine)

Submitted by

Kareem Mahmoud Ibrahim Abdou

Department of Biochemistry

University of Toyama

Contents

ACKNOWLEDGEMENTS

First of all, I would like to thank Prof. Kaoru Inokuchi for supervising me throughout my Ph.D. study. When I arrived in Japan on January 2014, I did not have enough knowledge about neuroscience, but his guidance and teaching helped me to overcome the difficulties and to acquire the knowledge. He has always been available, even when he was not in the lab. He lends me a hand to increase my self-confidence, to become independent, and to evolve as a scientist. I am thankful to him for his daily enthusiasm, sense of humour, and optimism. He gives me advices not only on the scientific level but also on the personal level and he showed us how to manage a big laboratory. I would also like to thank other two co-supervisors from University of Toyama, Prof. Hisao Nishijo and Associate Prof. Michihisa Tohda. Also, I would like to thank Prof. Shin-ichi Muramatsu, Mika Ito and Naomi Takino, Jichi Medical University for providing us with the AAV vectors. I would like to thank Dr. Mohammad Shehata, California Institute of Technology, for his support during the doctoral course, especially in the first grade. He helped me a lot in establishing my life in Japan and taught me basic experiments. Moreover, I am grateful to Dr. Ali Elhalawany, Ahmed Shehata, Khaled Ghandour, Mohamed Hussein, Maha Wally, Ali Choucry, Mohamed Ibrahem, Sherif Abdelhameed, Sherif Arafa, Magdy Saif, Samar Imbaby, Alaa Refaat and Heba Emam for their wonderful support and company. Special thanks to Khaled Ghandour (Abo el khawaled), my companion who means a lot to me. I owe a lot to Dr. Akinobu Suzuki, Dr. Masanori Nomoto, Dr. Yoshitake Sano, Hirotaka Asai and Naoya Oishi for their help in my experiments and in translating the Japanese documents especially those for scholarships. I would also like to thank other members of Prof. Kaoru Inokuchi's laboratory for their support, fruitful discussion and suggestion regarding my research and for their good attitude. Countless appreciations to Dr. Noriaki Ohkawa and Dr. Masanori Nomoto for their moral support and for increasing my passion during my Ph.D. study. I would like to appreciate the help and guidance of Dr. Md Jahangir Alam. He guided me a lot

in establishing my life in Toyama. I am greatly thankful to the laboratory Secretary; she is very helpful and efficient and provided the required information and guided me to prepare the administrative and educational documents. Additionally, I am greedy to thank all of my friends at University of Toyama whom have passed all these years together. I am very much grateful to my parents and my brother for their uncountable spiritual support that allowed me to do my best here in Toyama. I would like to thank my colleagues in Egypt (Kareem Adel, Kareem Elebzary, Kareem Khedr, Kareem Ghareeb and Kamal Essam) for keeping in touch with me through the past 4 years and their endless support. Also, I would like to thank all my colleagues at the department of biochemistry, Cairo University (a7la mesa 3l nas l kwisa group) for their support and encouragement. Finally, I am grateful to Allah for all his blessings.

ABBREVIATIONS

AC: Auditory cortex

AFC: Auditory fear conditioning

AMPAR: α-amino-3-hydroxy-5-methyl4-isoxazolepropionic acid receptor

Ani: Anisomycin

AP: Anterior-posterior

Atg: Autophagy-related genes

BLA: Basolateral amygdala

CFC: Contextual fear conditioning

CS: Conditioned stimulus

EC: Entorhinal cortex

DG: Dentate gyrus

DAPI: 4,6 Diamidino-2-phenylindole

DV: Dorsal-ventral

FDA: Food and Drug Administration

fEPSP: Field excitatory postsynaptic potential

FS: Foot shock

GABAR: γ-aminobutyric acid receptors

hSyn: Human synapsin 1

IFN: Ifenoprodil

LA: Lateral amygdala

LC3: light chain protein 3

LTD: Long-term depression

LTM: Long-term memory

LTP: Long-term potentiation

MGm: Medial part of medial geniculate nucleus

ML: Medial-lateral

mTOR: mammalian target of rapamycin

NMDAR: N-methyl-D-aspartate receptor

NS: Non-shock

PBS: Phosphate buffered saline

PI3K: phosphatidylinositol-3-monophosphate kinase

PP: Perforant pathway

PTSD: Post-traumatic stress disorder

tBC: Tat-beclin

TFP: Trifluoperazine

TRE: Tetracycline responsive element

tTA: Tetracycline transactivator

US: Unconditioned stimulus

ABSTRACT:

Throughout the life, our brains form several memories that are encoded in specific neuronal ensemble, called engram cells. Some of these memories are associated and stored in shared ensemble. However, brain machinery that underlies memory storage and defines certain memory identity amidst numerous number of memories stored in the same ensemble is poorly understood. Here we show that autophagy contributes to fear memory destabilization through inhibiting autophagy activity in the amygdala. Then, we showed that autophagy induction can overcome a boundary condition of a resistant auditory fear memory which depended on AMPAR endocytosis. In contextual fear conditioning, autophagy induction in the amygdala, enhanced fear memory destabilization and when combined with anisomycin, complete retrograde amnesia was attained. Moreover, using auditory fear conditioning and c-fos-TetTag system, optogenetic stimulation of the activated ensemble terminals of auditory cortex (AC) and medial geniculate nucleus (MGm) in lateral amygdala (LA) after complete retrograde amnesia, failed to induce memory recall at recent and remote time points, indicating that memory engram no longer exists in that circuit. This result was correlated with the resetting of plasticity and functional connectivity between the engram assemblies. Furthermore, potentiating or depotentiating the plasticity at synapses specific to a given memory did not affect the linked memory that is encoded in the same ensemble, suggesting that memories are stored in specific synapses. These findings demonstrate that when two associative memories are encoded in shared ensemble, synapse specific plasticity delineates specific memory identity and that specific engram plasticity is both sufficient and crucial for information storage. Moreover, our study sheds light on the capability of selective and integral erasure of memory trace from the engram network, suggesting a potential way to treat post-traumatic stress disorder (PTSD).

INTRODUCTION:

Formation of long-term memory (LTM) is experimentally divided into several processes: acquisition, consolidation, retrieval, and reconsolidation (1, 2). During the acquisition process, newly acquired memories are kept only for the short term, in an unstable form. Consolidation is the process of stabilizing memories to be maintained as LTM. Protein synthesis inhibitors, such as anisomycin (Ani), interrupt memory consolidation and cause amnesia (3). Retrieval of LTM can induce a destabilization process that returns memories to a labile state, which is eventually followed by another protein synthesis-dependent reconsolidation process (4, 5). The reconsolidation process serves to strengthen or renew the original memory (6-9), indicating the importance of destabilization/reconsolidation processes in the fate of original memory.

Blocking reconsolidation has been suggested as a therapeutic tool to weaken traumatic memories in anxiety disorders such as post-traumatic stress disorder (PTSD) (10). However, these traumatic memories must be sufficiently destabilized in the first place, before their reconsolidation (restabilization) can be blocked, or even updated. The initial destabilization step is challenging in cases of PTSD, as memories are formed under extremely stressful conditions, and it would require pharmacological assistance (6, 10). In memory reconsolidation research, these conditions that constrain the memory from being destabilized after recall are called boundary conditions which include the age and strength of the memory and the reactivation strength (1). Existing evidence indicates that inhibition of synaptic protein degradation, namely the ubiquitin proteasome system, prevents memory destabilization (5).

Macro-autophagy, hereafter referred to as autophagy, is another major protein degradation pathway where a newly synthesized isolation membrane sequesters a small portion of the cytoplasm to form a multilamellar vesicle called an autophagosome. To degrade the entrapped contents, autophagosomes fuse into the endosome-lysosome system (11, 12). The

process of autophagosome synthesis is orchestrated by molecular machinery consisting of the autophagy-related genes (Atg) found in yeast, and their mammalian homologs (13, 14). Since the discovery of autophagy, diverse physiological and pathological roles of autophagy have been demonstrated in several body organs (11). In the brain, autophagy plays role in the elimination of misfolded-protein aggregates; hence it plays an important role in neurodegenerative diseases (12) and is essential for the development of a healthy brain (15-17).

Neurons may have adapted autophagy to suit their complex needs, allowing it to contribute to their synaptic function (11, 12, 18, 19). In line with this idea, autophagosomes are found not only in the neuron's soma and axons, but also in the dendrites (20, 21), and early evidence indicates that autophagy may function post-synaptically, as reported in the nematode *Caenorhabditis elegans*, where endocytosed γ-aminobutyric acid receptors (GABAR) are selectively targeted by autophagosomes (22). Depolarization or N-methyl-D-aspartate (NMDA)-induced long-term depression (LTD) stimulates autophagy in cultured neurons, which is accompanied by enhanced degradation of GluA1, an α-amino-3-hydroxy-5-methyl4-isoxazolepropionic acid receptor (AMPAR) subunit (21). Both GABAR and AMPAR play roles in the synaptic plasticity models of LTD and long-term potentiation (LTP), which are causally correlated with memory (23-25), suggesting that autophagy plays a role in synaptic plasticity and memory. The regulation of protein synthesis intersects with autophagy regulation at the mammalian target of rapamycin (mTOR) and the phosphatidylinositol-3-monophosphate kinase (PI3K). By careful consideration of the discrepancy in the effects of the mTOR and PI3K modulators on memory processes, prominently on the reconsolidation process (18, 26, 27), autophagy is suggested to play a pivotal role in memory destabilization and reconsolidation after retrieval (18). We hypothesize that autophagy plays a role in synaptic and memory destabilization. Also, autophagy induction can be utilized to overcome the reconsolidation boundary conditions.

Memories are stored throughout the brain in specific neuronal ensemble, called engram cells, which are activated during the corresponding event (28). Although multiple associated memories can be encoded in the same population of cells (29-32), they may remain distinct and each memory has its own identity (29). It has been thought that memories are formed by long term changes in the synaptic strength, a process known as synaptic plasticity (33-36). Recent studies demonstrated that synaptic plasticity is essential for the retrieval, but not the storage, of associative fear memories (37-41). However, the aforementioned studies did not show how the brain stores and defines a specific memory identity when two memories are encoded in the same ensemble, leaving the fundamental substrate for memory storage elusive.

RESULTS

To modulate autophagy activity with the time window of reconsolidation, we pharmacologically targeted the Beclin1 protein which is part of the Beclin1-Atg14L-Vps34 lipid kinase complex that is involved in autophagosome synthesis. Also, this will specifically modulate autophagy activity without affecting the endocytosis, mTOR, or PI3K activity (45-49). For autophagy induction, we used the cell-permeable tat-beclin1 peptide (tBC), which is composed of the human immunodeficiency virus-1 transduction domain attached to the necessary and sufficient peptide sequence of the beclin1 protein (47). The tBC peptide induces autophagy in the brains of mice neonates when systemically injected (47), and induces autophagy in the amygdala of adult mice when directly infused (Figure 1) as monitored through the conversion of the light chain protein 3 (LC3), an autophagosome-specific marker, from its inactive form (LC3-I) to the lipidated active form (LC3-II). For autophagy inhibition, we used Spautin-1 (Spautin), which promotes the degradation of the Beclin1-Atg14L-Vps34 complex through inhibiting the ubiquitin-specific peptidases that target the beclin1 subunit of the complex (49). Infusion of spautin into the amygdala inhibited both the basal and the tBC-induced autophagic activity (Figure 1).

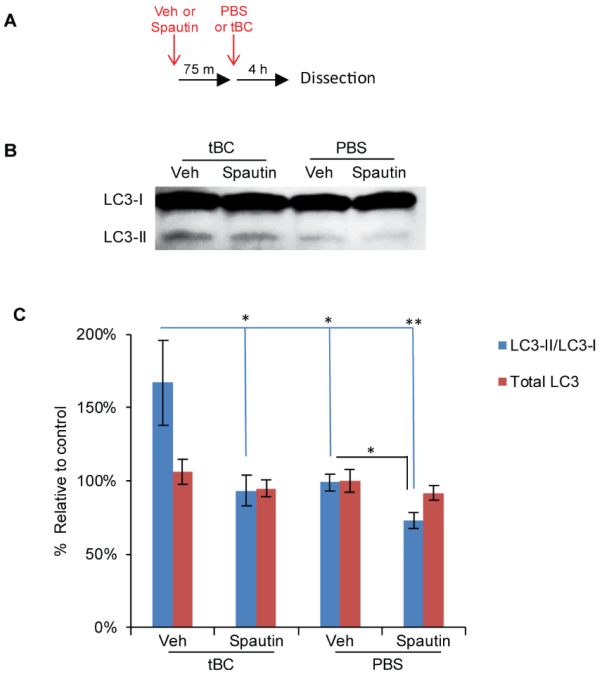

Figure 1. Autophagy modulation in adult mouse amygdala.

(A) Experimental design.

(B) Representative LC3 immunoblot from amygdala lysates. LC3, microtubule associated protein 1 light chain protein 3, is the mammalian homolog of Atg8 and exists in two forms: the inactive form (LC3-I) and the lipidated active form (LC3-II). LC3-II is an AP-specific marker as it is the only Atg remaining on the AP membrane after maturation.

(C) Quantitation of the signal intensity represented as percentage relative to a Veh/PBS sample (n = 4 per group; one-way ANOVA, LC3-II/LC3-I: P = 0.007 and Total LC3: P = 0.505; Tukey-Kramer multiple comparisons test). For within-group comparison of the PBS groups, unpaired Student's t-test was used. * P < 0.05; ** P < 0.01. Center values represent means. Error bars represent mean ± standard error of mean (s.e.m.). PBS: phosphate buffered saline; tBC: Tat-beclin 1; Veh: vehicle for Spautin.

To examine the effect of autophagy modulation on memory destabilization, we employed a reconsolidation model of fear conditioning. Fear conditioning is an associative learning paradigm, in which animals learn to associate a specific auditory cue (auditory fear conditioning, AFC) or context (contextual fear conditioning, CFC), which is a conditional stimulus (CS), with a foot shock, an unconditional stimulus (US). When animals are subjected to the CS, they recall the fear memory, resulting in a freezing response.

When a one tone-footshock pair (1FS-AFC) was used for conditioning in the AFC paradigm, Ani infusion into the lateral amygdala (LA) after tone retrieval led to a significant decrease in the tone-elicited freezing response compared with the PBS-infused group (Figure 2A-C), in agreement with previous reports (4, 50, 51). Inhibiting autophagy through spautin infusion into the LA before retrieval partially blocked the Ani amnesic effect, indicating that autophagy contributes to the memory destabilization process (Figure 2A-C).

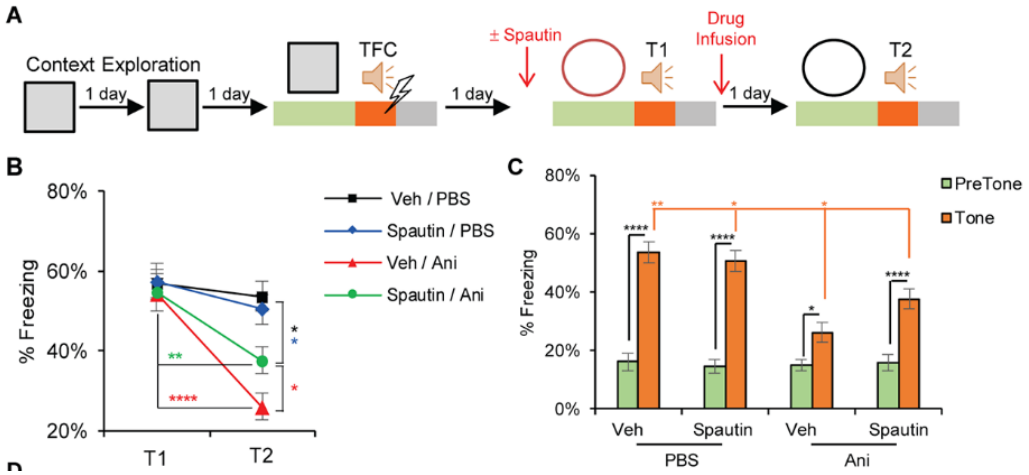

Figure 2. Autophagy contributes to fear memory destabilization.

(A) Design for the one tone-footshock pair auditory fear conditioning (1FS-AFC) experiments. For autophagy inhibition, Spautin was injected before T1 or Veh as control. For autophagy induction, tBC was injected after T1 and there were no injections before T1. Lime green bars, pre-tone; orange bars, during tone; gray bars, after tone.

(B) Average percentage freezing during tone at T1 and T2 showing that blocking autophagy significantly decreased the amnesic effect of Ani (Two-way ANOVA, F = 4.224, P = 0.0115; Bonferroni's post-hoc test, within group comparison; Newman-Keuls test, between groups comparison).

(C) Average percentage freezing during tone at T2 (as in B) was compared with the pre-tone freezing levels (n = 10 mice/ group except for Spautin/Ani group (n = 11)); (Two-way ANOVA, F (3, 37) = 9.923, P < 0.0001; Bonferroni's post-hoc test).

Next, we examined the effect of autophagy induction on stronger, boundary condition, AFC training. We generated a boundary condition by increasing memory strength using three tone-FS pairs (3FS-AFC). In the 3FS-AFC, Ani infusion into the LA after retrieval did not show any significant effect on the tone-elicited freezing response in comparison with the vehicle-infused group. By contrast, Ani+tBC infusion after retrieval reduced the tone-elicited freezing

response to pre-tone levels, indicating that autophagy induction enhances memory destabilization beyond a fear memory boundary condition (Figure 3A-C). Without the retrieval session, Ani+tBC administration in the 3FS-AFC had no effect on auditory fear memory (Figure 3C), indicating that a retrieval-specific process is necessary for the autophagy-enhancing effect on memory destabilization. Interestingly, tBC administration alone after retrieval did not demonstrate any amnesic effect (Figure 3B, C). Collectively, the results obtained from both the inhibition and the induction of autophagy indicate a causal relationship between autophagy and memory destabilization.

We attempted to elucidate how autophagy modulates memory destabilization. As AMPAR are endocytosed after memory retrieval, we hypothesized that the autophagosome may fuse with endosomes carrying AMPAR and dictate their fate to lysosomal degradation (18, 21, 52). Blocking endocytosis would block the autophagy effect on memory destabilization. The neural activity-dependent endocytosis of AMPAR relies on the carboxy-tail of GluA2, and the use of the synthetic peptide Tat-GluA2$_{3Y}$ is well-established in attenuating activity-induced, but not constitutive, GluA2-dependent synaptic removal of AMPARs (53-56). In the 3FS-AFC, Tat-GluA2$_{3Y}$ peptide infusion into the LA before retrieval completely blocked the Ani+tBC amnesic effect, while the control mutant peptide Tat-GluA2$_{3A}$ had no effect (Figure 3A, D, E). These data indicate that AMPAR endocytosis is upstream to the autophagy induction effect on enhancing memory destabilization.

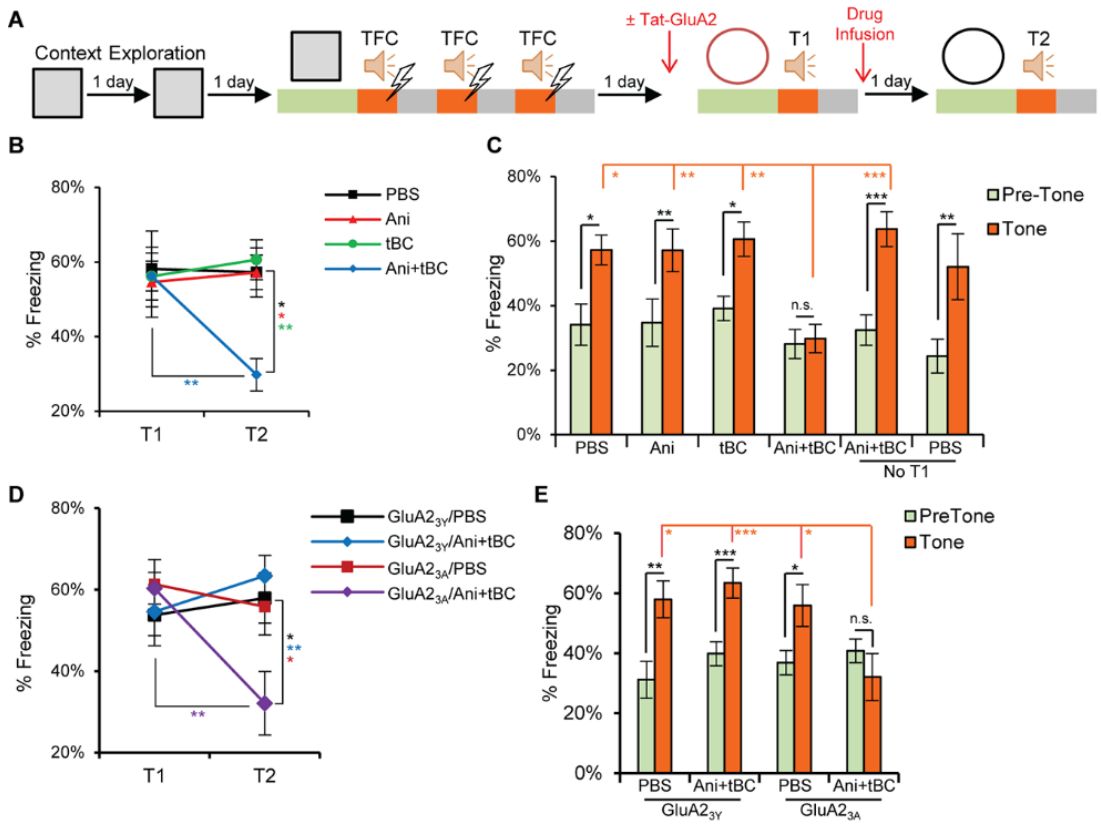

Figure 3. Autophagy overcomes a reconsolidation boundary condition that is AMPAR endocytosis-dependent.

(A) Design for the three tone-FS pairs auditory fear conditioning (3FS-AFC) experiments as a reconsolidation the boundary condition. The experiment was carried out either with no injection before T1 or with injection of Tat-GluA2 peptides: GluA2$_{3Y}$, for blocking AMPA receptor endocytosis, or GluA2$_{3A}$, as a negative control. Lime green bars, pre-tone; orange bars, during tone; gray bars, after tone.

(B) Average percentage freezing during tone at T1 and T2 showing that autophagy induction combined with Ani showed significant retrograde amnesia while Ani alone showed no amnesic effect. PBS (n = 7), Ani (n = 9), tBC (n = 8), Ani+tBC (n = 10); (Two-way ANOVA, F (3, 30) = 3.476, P = 0.0281).

(C) Average percentage freezing during tone at T2 (as in B) was compared with the pre-tone freezing levels. NoT1 indicates that the drug infusion took place in a separate room

without T1 (no reactivation). PBS (NoT1) (n = 6), Ani+tBC (NoT1) (n = 8); (Two-way ANOVA, F (5, 42) = 2.77, P = 0.0299).

(D) Average percentage freezing during tone at T1 and T2 showing that blocking AMPAR endocytosis abolished the amnesic effect of autophagy induction. GluA23Y/ PBS (n = 8), GluA23A/ PBS (n = 9), GluA23Y/Ani+tBC & GluA23A/Ani+tBC (n = 11); (Two-way ANOVA, F (3, 35) = 4.787, P = 0.0067).

(E) Average percentage freezing during tone at T2 (as in D) was compared with the pre-tone freezing levels; (Two-way ANOVA, F (3, 35) = 7.616, P = 0.0005). Data are presented as mean ± s.e.m.; * *P* < 0.05; ** *P* < 0.01; * *P* < 0.001; **** *P* < 0.0001; Bonferroni's post-hoc test was used for within group comparison, while Tukey's test was used for between groups comparison, n.s. = not significant. Ani: anisomycin; PBS: phosphate buffered saline; tBC: Tat-beclin 1.**

We further investigated the autophagy induction effect on CFC as another reconsolidation paradigm. In CFC, the CS is a specific context, and the memory of the details of that context triggers a freezing response that is greater than that triggered by any other distinct context (57). Typically, inhibition of protein synthesis after CS retrieval leads to a certain degree of retrograde amnesia (6, 7). To assess the degree of the retrograde amnesia, we compared it with that of a reference group exposed to the same contexts without receiving any shock (NoFS). After CFC, an Ani infusion into the baso-lateral amygdala (BLA) after memory retrieval led to a decrease in the freezing response in comparison with the vehicle-infused group (Figure 4A, B) (50, 51). Nevertheless, the freezing response after Ani administration was significantly higher than that in the NoFS group, in both the specific and distinct contexts, implying that the resultant retrograde amnesia was only partial. After Ani+tBC administration, the average freezing response dramatically reduced, reaching no statistical significant difference from the

NoFS group in both contexts (Figure 4B). In addition, we assessed the complete amnesia for each mouse. In the Ani+tBC administered group, 5 out of 12 mice were regarded as completely amnesic, in contrast with only 1 out of 12 mice in the Ani administered group (see Methods for definition of complete amnesia) (Figure 4C, D). The completely amnesic mice did not differ from those in the NoFS group regarding the averaged freezing response (Figure 3E). When the completely amnesic mice were subjected to a reconditioning session, they regained the freezing response to levels matching the pre-amnesic freezing levels, indicating an intact capacity for fear expression (Figure 4E). As with AFC reconsolidation, tBC administration alone after retrieval did not demonstrate any amnesic effect (Figure 4B, C). Altogether, these behavioral data indicate that induction of autophagy enhanced the amnesic effect of protein synthesis inhibition after retrieval and resulted in an unprecedented level of retrograde amnesia.

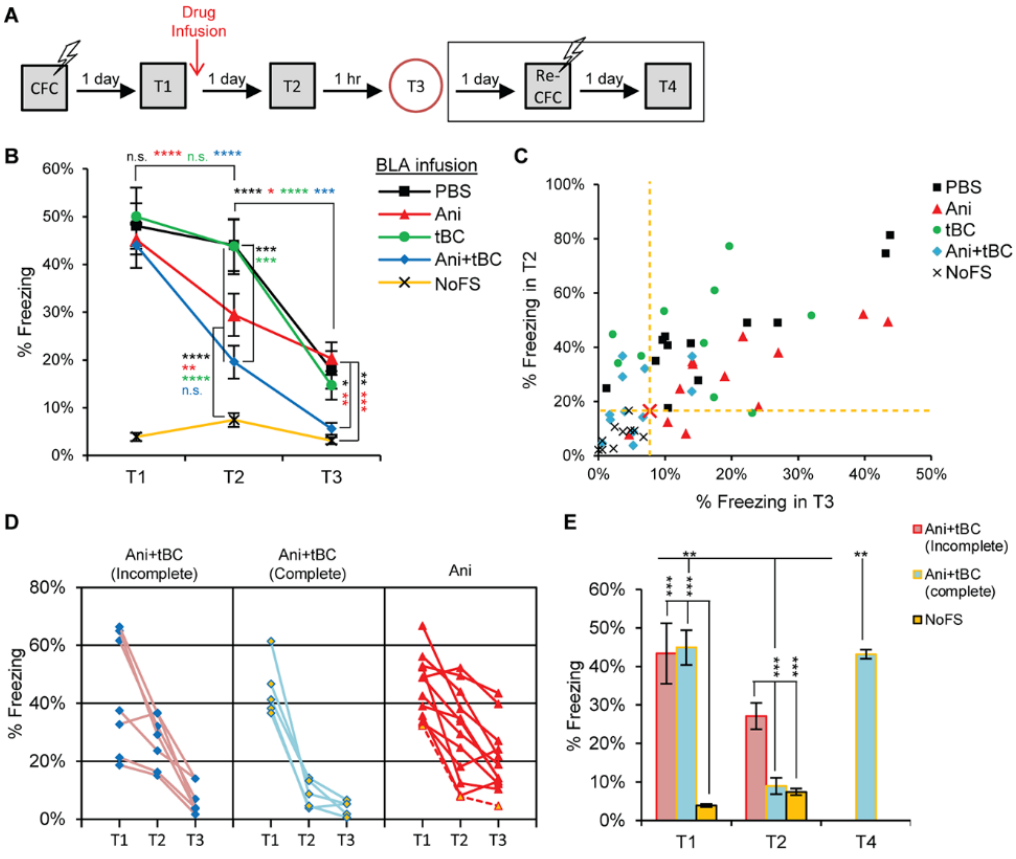

Figure 4. Autophagy enhances fear memory destabilization in contextual fear conditioning (CFC) when targeted to amygdala.

(A) Design for the CFC reconsolidation and reconditioning experiments.

(B) Average percentage freezing during retrieval (T1), and after the drugs were infused into the BLA when tested in the conditional stimulus context (T2) and in a distinct context (T3). Freezing levels at both T2 and T3 showed a significant enhancement of Ani amnesic effect when combined with autophagy induction. PBS, Ani & Ani+tBC (n = 12 mice / group), tBC & NoFS (n = 10 mice / group); (Two-way ANOVA, F (8, 102) = 10.19, P < 0.0001; One-way ANOVA, T3: P = 0.0001; Bonferroni's post-hoc test, within group comparison; Tukey's test, between groups comparison).

(C) Plots of individual mice freezing level at T2 against their freezing level at T3, for the assessment of complete fear amnesia after CFC. The red cross and yellow dashed lines represent a hypothetical point calculated from double the standard deviation for the freezing of the NoFS group at T2 and T3, where most of mice received the Ani+tBC treatment behaved as the NoFS group.

(D) Individual data for the complete and incomplete amnesic mice of the Ani+tBC group compared with the Ani one. The dashed red line is a complete amnesic mouse in Ani group.

(E) Average percentage freezing for the complete and incomplete amnesic mice of the Ani+tBC group compared with the NoFS group. The complete amnesic mice showed a normal freezing response one day after a reconditioning session (T4). Incomplete (n = 7), complete (n = 5), NoFS (n = 10); (One-way ANOVA, T1: P < 0.0001, T2: P < 0.0001, within Ani+tBC complete: P = 0.0021; Tukey's post-hoc test). Data are presented as mean ± s.e.m; * *P* < 0.05; ** *P* < 0.01; * *P* < 0.001; **** *P* < 0.0001; n.s. = not significant. Ani: anisomycin; BLA: baso-lateral amygdala; NoFS: no foot shock; PBS: phosphate buffered saline; tBC: Tat-beclin 1.**

Recently, it has been reported that after retrograde amnesia, memory engram cells, lacking increased synaptic strength owing to blocking protein synthesis after reconsolidation, still retain memory as they can retrieve memory upon optogenetic stimulation (43). In our study, a complete return of rodent to the non-traumatic behavior were only achieved after enhancing destabilization. It is of interest to know whether the memory engram cells will still retain the ability to retrieve memories after complete retrograde amnesia, clarifying whether synaptic plasticity is a crucial component of the memory information storage. We utilized auditory fear conditioning (AFC) paradigm that employed two different tones (2kHz, 7kHz) to ask whether engram assemblies still keep the memory trace after the complete amnesia. First, we confirmed that mice can discriminate between these tones (Figure 5A, B). Mice were subjected to fear conditioning to 7kHz tone, then they were tested using 7kHz and different tone (2kHz) (Figure 5A). Mice showed higher freezing level in response to 7kHz tone only (Figure B), indicating that mice can discriminate between the two tones.

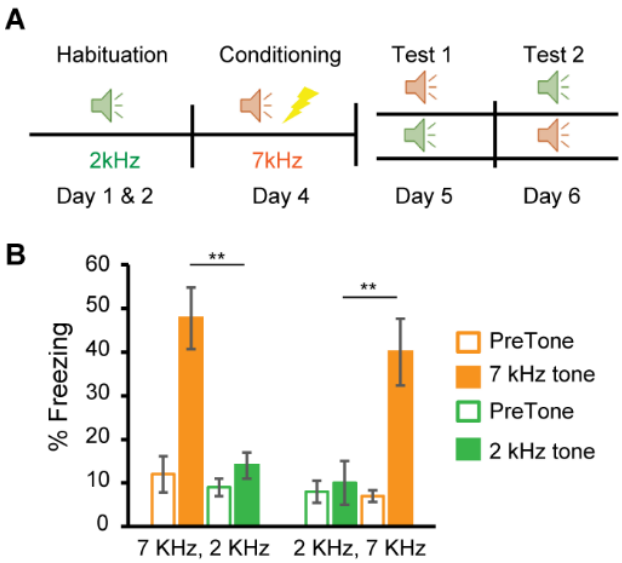

<u>Figure 5. Mice discriminate between 2kHz and 7kHz tones</u>.

(A) Design for the discrimination experiment, wild type mice were exposed to AFC and then they were divided into two groups, the first one received 7kHz tone in test 1 and 2kHz tone in test 2, while the second group received the opposite order.

(B) Freezing levels before and during the two tones (n = 11 mice / group). Statistical comparisons are done using paired t-test. * p < 0.05; ** p < 0.01. Data are represented as mean ± s.e.m.

Then, we injected adeno-associated virus (AAV) expressing Cre recombinase under the control of tetracycline-responsive element (TRE) in combination with AAV encoding DIO-oChIEF-citrine downstream of human synapsin 1 (hSyn) promoter in the auditory cortex (AC) and medial geniculate nucleus (MGm) of c-Fos/tTA transgenic mice to label the activated ensemble with oChIEF (Fig. 6F, G). We confirmed also that 2kHz & 7kHz tones activated different neuronal populations in AC (Figure 6A-E). Mice were exposed to AFC after doxycycline withdrawal (OFF DOX) and one day later, they were infused with PBS, Anisomycin (Ani) and Ani+tBC in lateral amygdala (LA) immediately after test session. Ani infusion induced partial retrograde amnesia, while combining Ani with tBC accomplished complete amnesia as the freezing level was comparable to that of non-shock (NS) and unpaired control groups (Fig. 6H, I). Optogenetic activation of the axonal terminals of AC & MGm engram cells in LA induced fear memory recall in PBS and Ani groups, which is consistent with previous study[17], whereas it failed in the Ani+tBC-treated mice (Fig. 6J). These results indicate that AC-LA & MGm-LA engram circuits no longer store memory information after complete amnesia.

Since Ani partially disrupts the enhanced synaptic strength in engram cells (43), we expected that induction of optical LTP in Ani group, but not in Ani+tBC group, would revive the capability of memory retrieval by natural cue. Indeed, after optical LTP, Ani-treated mice were completely recovered from amnesia and the freezing level was not significantly different from PBS-treated mice, whereas Ani+tBC-treated mice showed partial reinstatement in memory performance as their freezing level was slightly increased, but still significantly lower

than PBS group. The slight increase in the freezing level of Ani+tBC group after LTP induction was similar to that of the unpaired group, which did not form associative memory, suggesting that this increase was due to building an associative memory rather than restoring previously stored memory (Fig. 6K). To check whether LTP had non-specific effects and would lead to memory generalization, mice were tested with a different tone and they did not exhibit generalization (Fig. 6K). Then, we conducted remote memory test to examine the persistence of memory erasure, and we found that unlike Ani group that showed spontaneous memory recovery, Ani+tBC group displayed significantly lower freezing than Ani & PBS groups in both natural cue and optogenetic tests, indicating that memory erasure was long-lasting and the memory did not undergo spontaneous recovery by time (Fig. 6L, M). Ani+tBC-treated mice that received LTP showed light-induced freezing comparable to that of PBS group in Test 9, excluding the possibility of LA damage by Ani+tBC treatment. Furthermore, the previous results were reproduced when we labelled and manipulated the engram cells in LA (Figure 7).

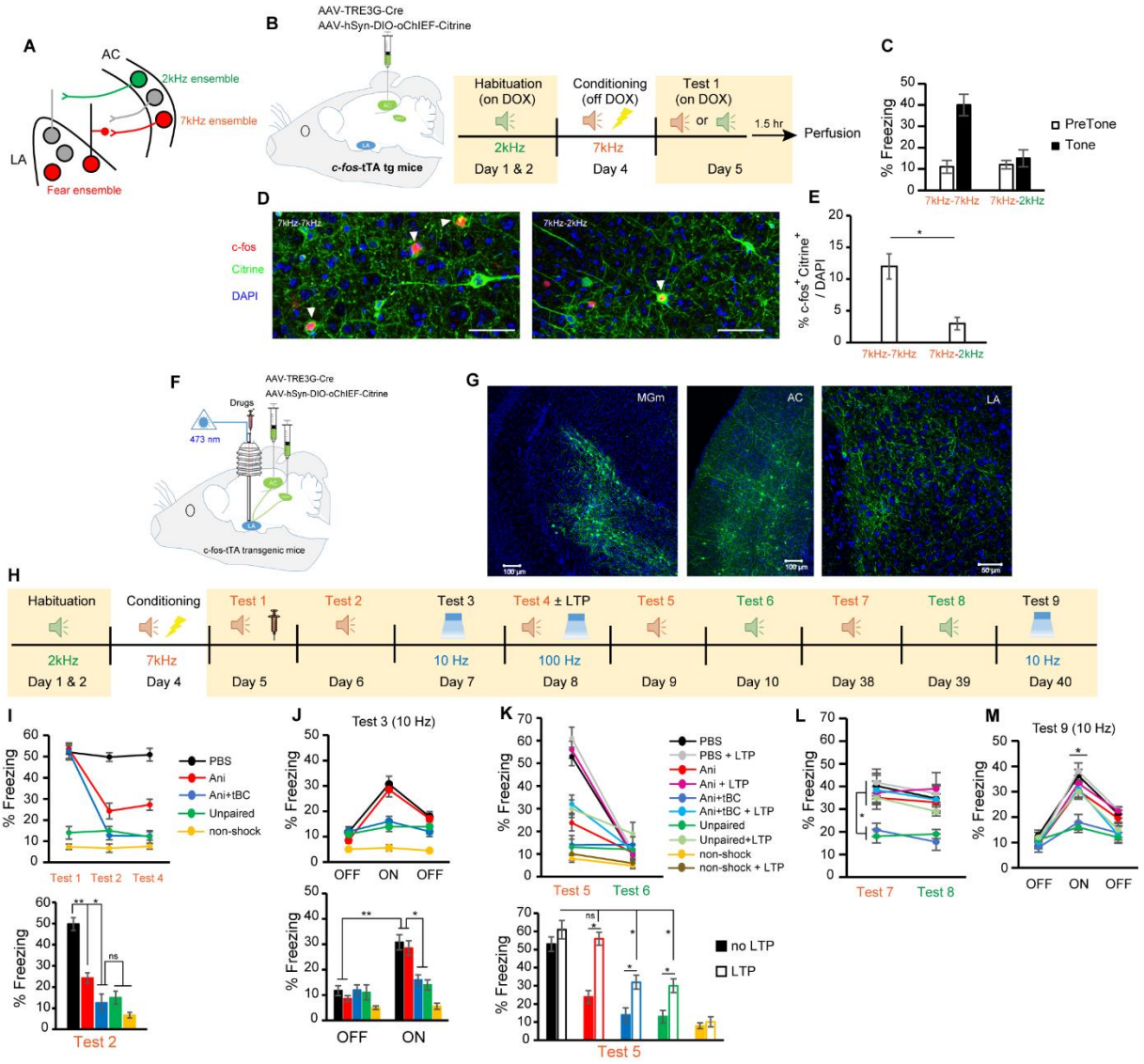

Figure 6. Integral and long-lasting erasure of fear memory trace from AC-LA and MGm-LA engram circuits.

(A) Model showing the ensemble responsive for the 2kHz and 7kHz tones in AC and the fear-responsive ensemble in LA.

(B) Experimental design to label the 7kHz and 2kHz-responsive ensemble in AC with citrine and c-Fos, respectively.

(C) Freezing levels before and during 7kHz and 2kHz tones presentation in test session.

(D) Representative images showing two different ensembles encoding different tones.

(E) c-Fos$^+$/ citrine$^+$ overlap cell counts (*n* = 4 mice / group). Statistical comparisons are done using unpaired *t*-test. * $p < 0.05$. Data are represented as mean ± s.e.m.

(F) Labelling strategy for the AFC-responsive ensemble in AC and MGm using c-Fos/TetTag system.

(G) Expression of oChIEF in AC, MGm neurons and their axonal terminals in LA.

(H) Design for memory engram erasure experiment.

(I-M), Freezing levels before and after drug injection (I), during 10 Hz stimulation (J), in response to the conditioned and neutral tones after optical LTP (K), at remote time point (L), during 10 Hz stimulation at remote time point (M). n = 20 mice / group (I, J); n = 10 mice / group (K-M). I-K, Bottom, statistical significance between groups during test 2 (I), during light-off and light-on epochs (J), during test 5 (K). Statistical comparisons are done using one-way ANOVA (I, K, L); two-way ANOVA (J, M). * p < 0.05; ** p < 0.01. Data are represented as mean ± s.e.m.

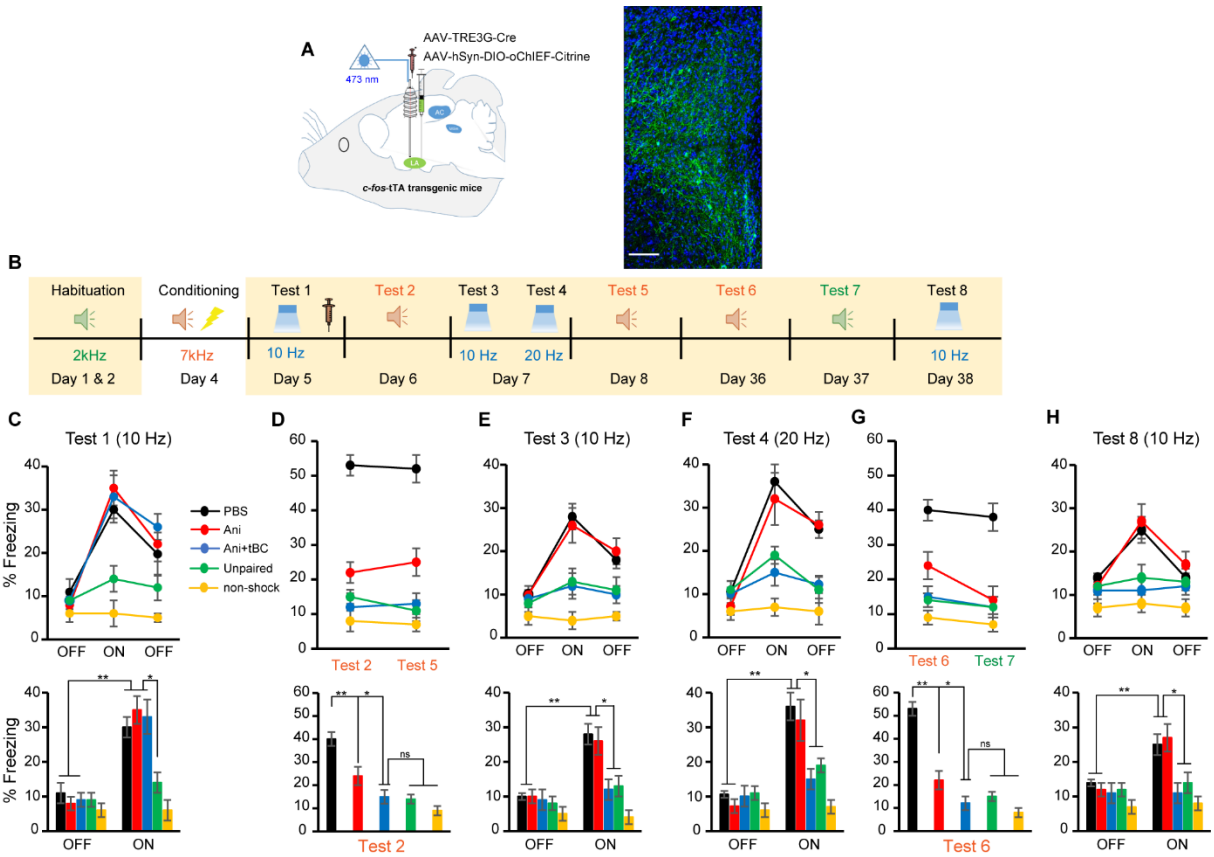

Figure 7. LA engram cells no longer store the memory after complete amnesia.

(A) Left, labelling strategy for the AFC-responsive ensemble in LA using c-Fos/TetTag system. Right, expression of oChIEF in LA neurons. Scale bar, 100 um.

(B) Experimental design for erasure of memory engram.

(C-H) Top, freezing levels during fear memory recall by 10 Hz stimulation (C), in response to the conditioned tone (D), during 10 Hz stimulation (E), during 20 Hz stimulation (F), in response to the conditioned tone and neutral tone at remote time point (G), during 10 Hz stimulation at remote time point (H). Bottom, statistical significance between groups (*n* = 10 mice / group). Statistical comparisons are done using one-way ANOVA (D, G); two-way ANOVA (C, E, F, H). * $p < 0.05$; ** $p < 0.01$. Data are represented as mean ± s.e.m.

To confirm that optical LTP protocol was producing the expected synaptic response, we carried out in vivo recording in the LA of anaesthetic mice. Light pulses at 0.033Hz to the terminals of AC & MGm engram cells produced in vivo field response which was potentiated by optical LTP protocol (Figure 8A, B).

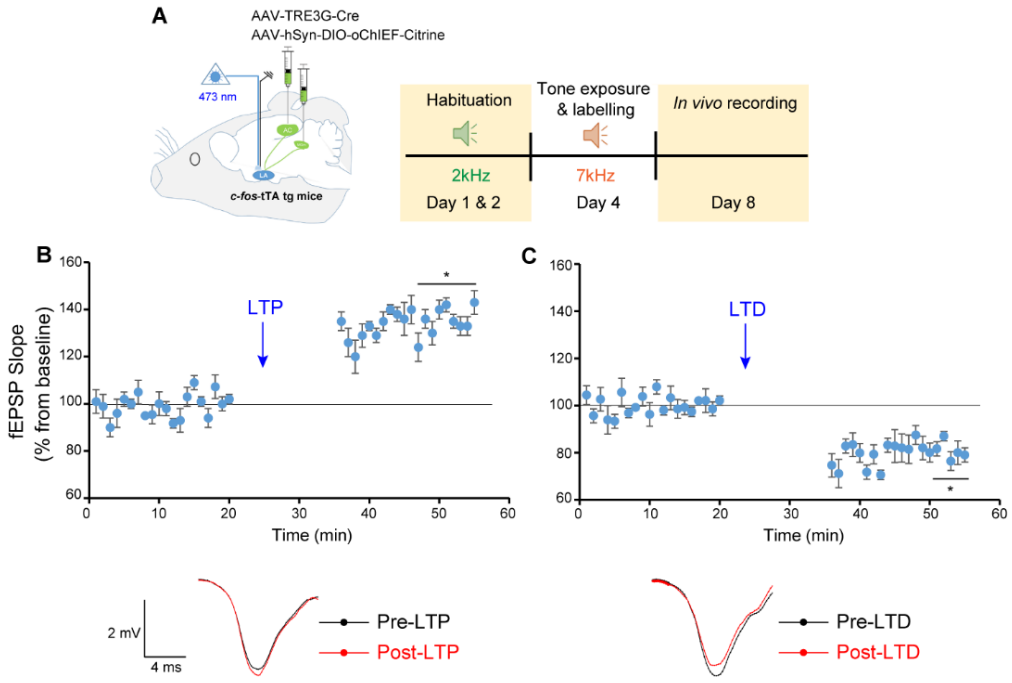

Figure 8. *In vivo* induction of optical LTP and LTD.

(A) Experimental design.

(B) Top, average of in vivo field EPSP slope (normalized to baseline) before and after LTP induction (n = 4 mice / group). Bottom, representative traces before (black) and after (red) the stimulation protocol. Scale bars, 2 mV, 4 ms.

(C) Top, average of in vivo field EPSP slope (normalized to baseline) before and after LTD induction (n = 4 mice / group). Bottom, representative traces before (black) and after (red) the stimulation protocol. Scale bars, 2 mV, 4 ms.

Statistical comparisons are done using two-way repeated measures ANOVA. * $p < 0.05$; ** $p < 0.01$. Data are represented as mean ± s.e.m.

To examine the mechanism underlying the complete memory erasure, we checked the synaptic plasticity in the affected network by LTP occlusion experiment in which artificial induction of LTP is occluded in circuits with potentiated synapses, while it is facilitated in circuits with unpotentiated synapses (58-60). One day after Test 1 (Figure 9A, B) and drug injection, in vivo recording was performed and we found that after LTP induction the degree of potentiated synaptic response in Ani+tBC group was higher than that of PBS and Ani groups (Figure 9C, D). Remarkably, there was no significant difference in the potentiated synaptic response between Ani+tBC group and non-shock group. These results suggest that synaptic plasticity might be totally reset after complete amnesia returning to non-shock level, while it was partially disrupted in Ani group. Then, we measured the connectivity pattern between upstream and downstream engram cells after integral memory erasure. Engram cells in LA were labelled with mCherry, the axonal terminals of AC & MGm engram cells were optogenetically stimulated and the overlap between $mCherry^+$ cells and $c\text{-}Fos^+$ activated cells was counted (Figure 9E-G). Complete amnesia resulted in significant decrease in the $c\text{-}Fos^+/mCherry^+$

overlap as compared to PBS and Ani groups (Figure 9H), which is consistent with the behaviour data and the total resetting of synaptic strength.

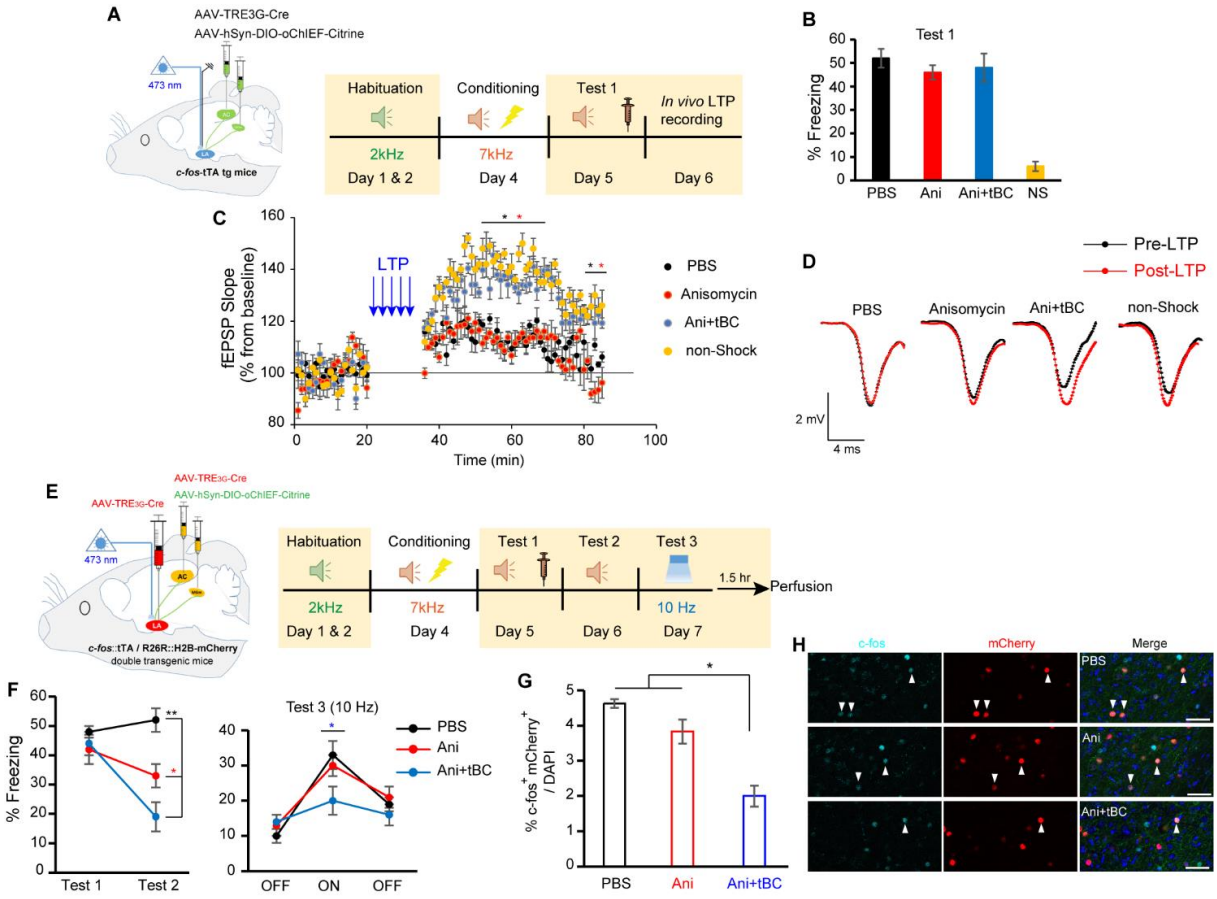

Figure 9. Resetting of synaptic plasticity and functional connectivity between engram assemblies as neural correlates of complete amnesia.

(A) Left, labelling strategy. Right, experimental design.

(B) Freezing level during test 1.

(C) Average of *in vivo* field EPSP slope (normalized to baseline) before and after LTP induction (two-way repeated measures ANOVA, *n* = 4 mice / group).

(D) Representative traces before (black) and after (red) optical LTP induction. Scale bars, 2 mV, 4 ms.

(E) Left, labelling of engram assemblies in AC, MGm and LA using double transgenic mice (c-Fos::tTA/R26R::H2B-mCherry). Right, experimental design.

(F) Freezing levels during test 1, test 2 and test 3 (one-way ANOVA).

(G) c-Fos$^+$/ mCherry$^+$ overlap cell counts (one-way ANOVA, *n* = 4 mice / group). DAPI, 4′,6-diamidino-2-phenylindole. * *p* < 0.05; ** *p* < 0.01. Data are represented as mean ± s.e.m.

(H) Representative images showing c-Fos$^+$/ mCherry$^+$ overlap in LA, indicated by arrows.

Since memories are stored in interconnected networks and the brain can store two memories in shared ensemble (30, 33), we asked whether memories stored in the same ensemble would have the same identity, and hence, the same fate after completely erasing one of them. To answer this question, we tested the selectivity of our manipulation by utilizing two different auditory fear conditioning paradigms, separated by 5 hours to confirm that they will recruit overlapping ensembles in LA. First, we confirmed that 5 hours ON DOX were enough to stop the oChIEF expression (Figure 10). Then we checked the overlapping ensembles in LA and AC and we found that majority of LA engram cells for the first event (memory1) encoded the second event (memory2), whereas both memories were encoded in two distinct populations in AC (Figure 11A-E). Then, we used c-Fos/TetTag system to label neural ensemble activated in AC and MGm specifically during memory1 with oChIEF (Figure 11F), after 5 hours ON DOX, mice were exposed to memory2, then they were divided into two groups, the first one received PBS after memory1 retrieval and Ani+tBC after memory2 retrieval (gp1), and the second group received the vice versa (gp2). In gp1, memory2 only was erased by Ani+tBC while memory1 was preserved. Although memory1 in gp2 was disrupted, revealed by lower freezing level in test2, memory2 was not affected, signifying the selectivity of memory erasure (Figure 11G, I). Moreover, optogenetic stimulation of presynaptic terminals of engram cells corresponding to memory1 induced freezing response in gp1, but not in gp2 although in both groups, neurons storing both memories were affected by Ani+tBC treatment (Figure 11H). These results reveal

synapse specific engram erasure and indicate that memories, stored in shared engram cells, are synapse specific, and hence, have different fate.

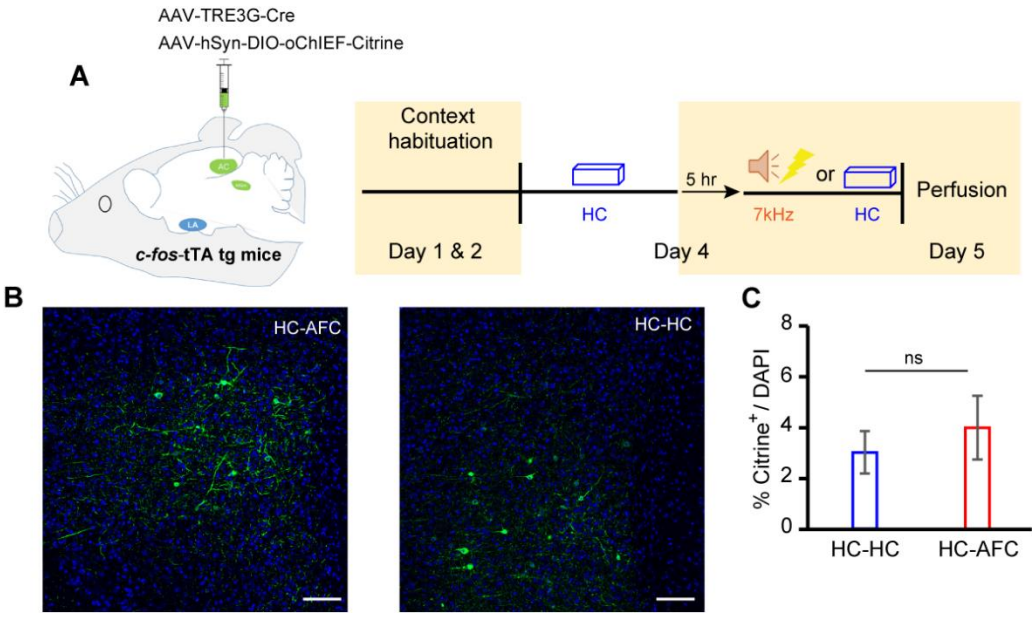

Figure 10. Five hours ON DOX are enough for stopping the expression of oChIEF.

(A) Experimental design, after 2 days without doxycycline (DOX) in food, mice were put back on DOX for 5 hours, then they either were exposed to AFC or stayed in their home cage. One day later, they were perfused.

(B) Representative images showing oChIEF-citrine expression after AFC while mice were ON DOX chow (1 g kg^{-1}). Scale bar, 100 um.

(C) oChIEF-citrine cell counts (unpaired *t*-test, $n = 4$ mice / group). * $p < 0.05$. Data are represented as mean ± s.e.m.

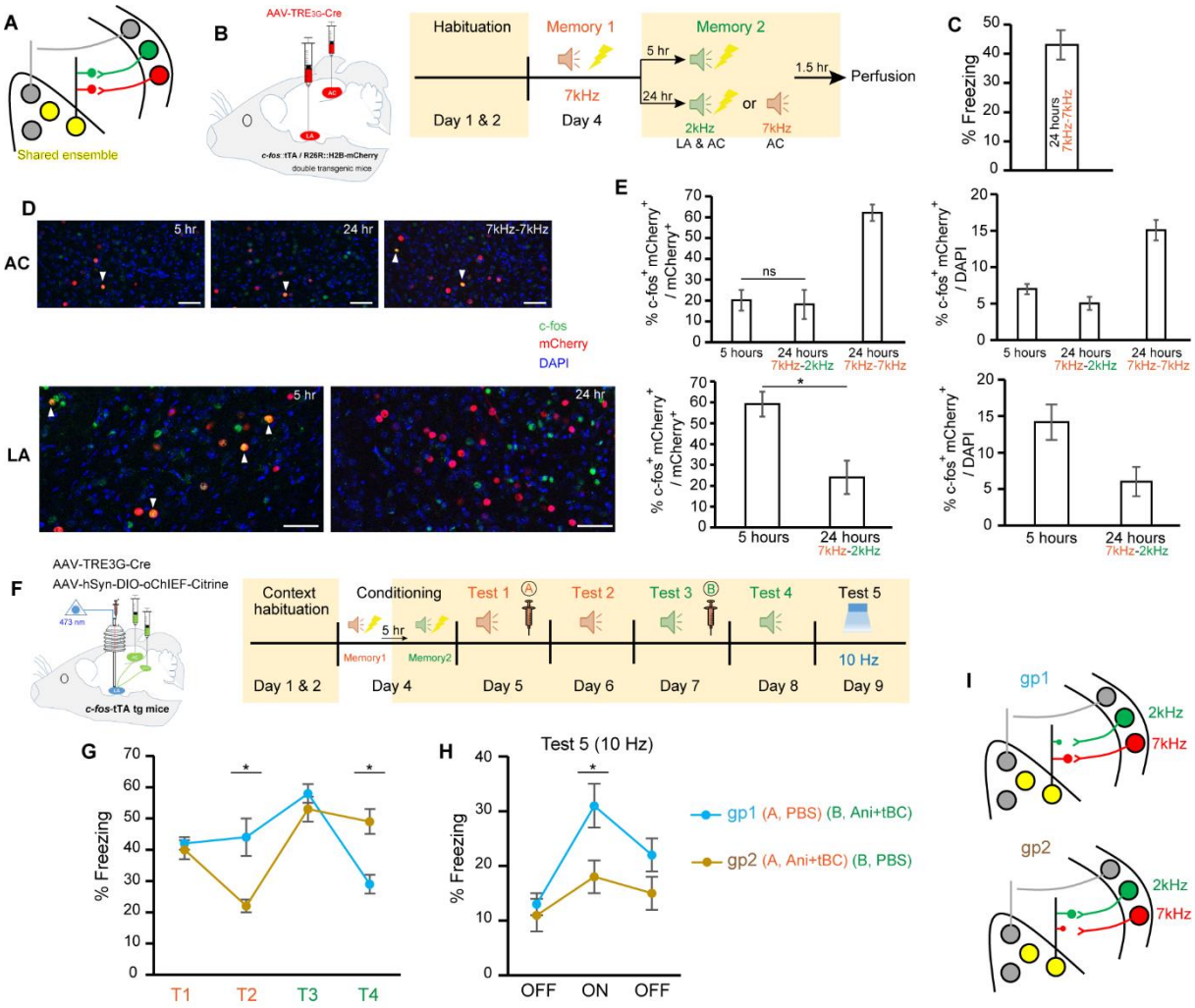

Figure 11. Synapse specific erasure of fear memory trace.

(A) Summary model for the neuronal ensemble in LA and AC after two associative memories encoded at 5 hours interval.

(B) Left, strategy to label engram cells in AC and LA using double transgenic mice (c-Fos::tTA/R26R::H2B-mCherry), injected with AAV-TRE$_{3G}$-Cre. Right, experimental design to check the overlapping ensembles between two associative memories that were encoded at different time intervals.

(C) Freezing level during 7kHz test session in the 7kHz-7kHz group.

(D) Top, representative images for the overlapping ensembles (arrow head) in AC. Bottom, same as top, but in LA.

(E) Top, c-Fos$^+$/ mCherry$^+$ overlap cell counts in AC (one-way ANOVA, *n* = 4 mice / group). Bottom, same as top, but in LA (unpaired *t*-test, *n* = 4 mice / group).

(F) Design for selective memory erasure experiment.

(G, H) Freezing levels for gp1 and gp2 during 7kHz and 2kHz tones before and after drug injection (G), during light-off and light-on epochs (H) (unpaired t-test, *n* = 10 mice / group). T1, test 1; T2, test 2; T3, test 3; T4, test 4. * $p < 0.05$; ** $p < 0.01$. Data are represented as mean ± s.e.m.

(I) Model for selective erasure of either 7kHz fear memory (red) or 2kHz fear memory (green), overlapped ensemble are in yellow.

To test how the associated memories are represented as individual identity within the shared ensemble and to dissect the fundamental mechanism underlying memory storage, we depotentiated the plasticity in synapses specific for memory1 by optical long term depression (LTD) (Figure 8A, C) and then we tested both memories (Figure 12A, B). Mice that received LTD showed freezing deficits in response to 7kHz tone only, but not 2kHz tone, as compared to control group that did not receive LTD (Figure 12C). Optogenetic stimulation to the terminals of the ensemble responding to 7kHz fear memory triggered light-specific freezing in the control group, while it failed in the LTD group although the 2kHz fear memory in the ensemble was intact (Figure 12D), indicating that selective depotentiation of synaptic plasticity deconstructed specific connectivity between engram assemblies. The previous results reveal that affecting neuron's synaptic inputs conveying specific memory information doesn't disrupt other synaptic memory in the same neuron. Next, gain of function experiment was performed by erasing both memories with Ani+tBC, then plasticity was restored in memory1-specific synapses by optical LTP (Figure 12E, F). Mice that received LTP protocol displayed higher freezing level in response to 7kHz tone only, while freezing response during 2kHz tone was unaffected (Figure

12G). Altogether, these findings demonstrate that synapse specific plasticity is necessary and sufficient for memory information storage and it delineates memory trace uniqueness, advocating the plasticity as a substrate for fear memory engram. Furthermore, these results suggest that synaptic plasticity can build specific connectivity within engram assemblies and that connectivity is a reflection of enhanced synaptic strength rather than an independent mechanism for memory storage.

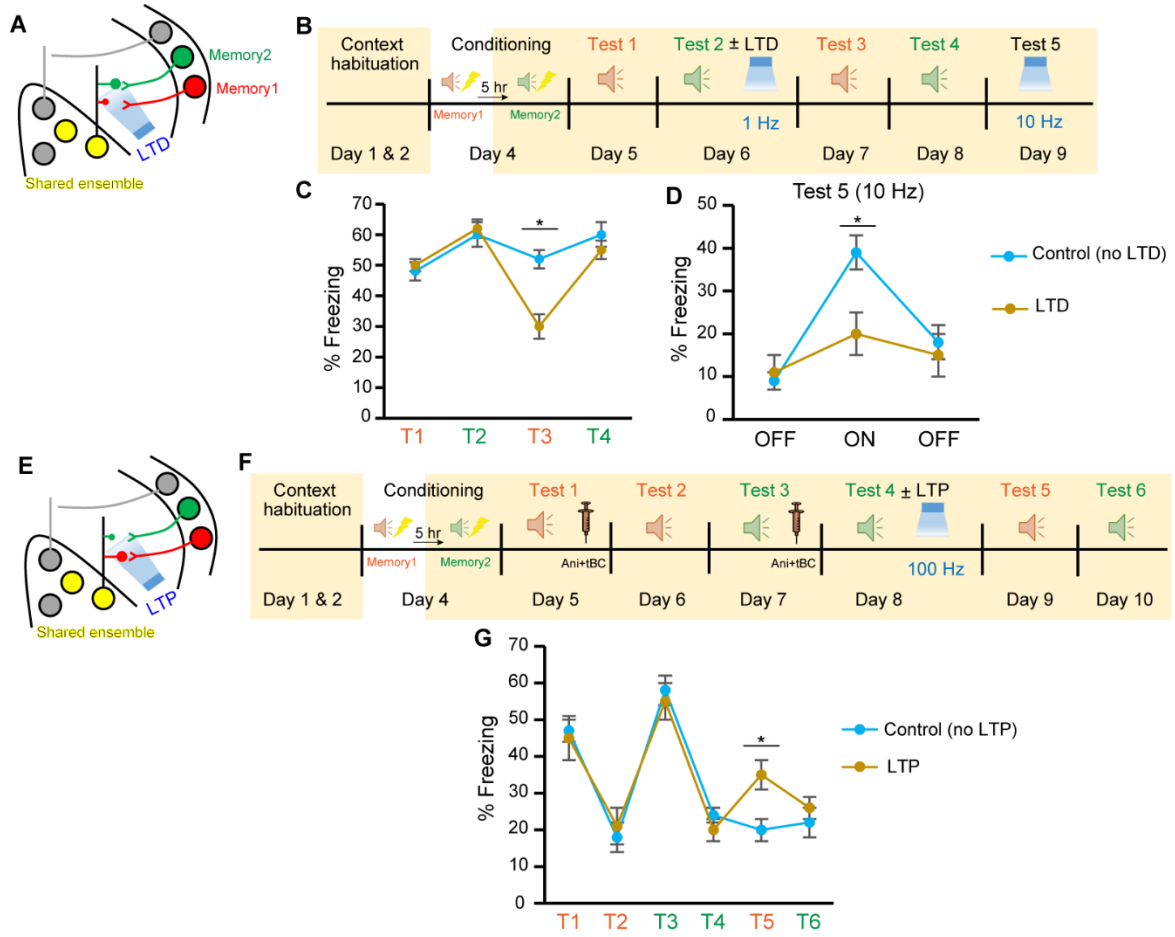

<u>Figure 12. Synapse specific plasticity is crucial for information storage and keeps the associated memories distinctive</u>.

(A) Summary model for synapse specific loss of function experiment.

(B) Design for loss of function experiment.

(C, D) Freezing levels in response to 7kHz and 2kHz tones before and after optical LTD induction (C), in response to optical stimulation (D) (*n* = 10 mice / group).

(E) Summary model for the gain of function experiment.

(F) Design for gain of function experiment.

(G) Freezing levels before and after complete amnesia and LTP induction (*n* = 10 mice / group). Statistical comparisons are done using two-way ANOVA. T1, test 1; T2, test 2; T3, test 3; T4, test 4; T5, test 5; T6, test 6. * $p < 0.05$; ** $p < 0.01$. Data are represented as mean ± s.e.m.

DISCUSSION:

Our results indicate that autophagy contributes to memory destabilization, and that its induction promotes both synaptic and memory destabilization, which is mediated through the degradation of the endocytosed AMPAR. Furthermore, autophagy induction overcomes a boundary condition rendering a fear memory pervious to reconsolidation. Moreover, memory engram cells no longer store the memory information after complete retrograde amnesia. Our study sheds light on the capability of selective and integral erasure of memory trace from the engram network, suggesting a potential way to treat post-traumatic stress disorder (PTSD). The findings presented here unravel how the brain organizes and stores multiple associative memories in shared ensemble, underpinning a causal relationship between synaptic input-specific plasticity and memory identity and storage.

Autophagy induction alone, through tBC administration after reactivation, did not show any significant amnesic effect in the 3FS-AFC and CFC. This indicates that, regardless of the degree of destabilization, if the protein synthesis is not compromised within a certain time window following reactivation, the synthesized proteins have the capacity to regain synaptic plasticity and memory. This demonstrates the capacity of protein synthesis in the restabilization of synapses and the reinstating of specific memories.

AMPAR are heterotetrameric complexes composed of various combinations of four subunits (GluA1–4), with the GluA1/2 and GluA2/3 tetramers being the two major subtypes (61). The amount of synaptic GluA2-containing AMPARs correlates with LTM maintenance and strength (62-65). Blocking the endocytosis of GluA2-containing AMPARs inhibits the induction of LTD, but not LTP, without affecting basal synaptic transmission (54, 56, 66, 67). More relevant is its involvement in memory destabilization, where it does not affect the acquisition or the retrieval of conditioned fear memory (52, 68). These reports are in agreement with our hypothesis that autophagy works through dragging endosomes carrying AMPAR to

lysosomal degradation, as evidenced by our demonstration that GluA2-dependent AMPAR endocytosis is a prerequisite for autophagy to affect memory destabilization. Additionally, GluA2-dependent AMPAR endocytosis correlates with the decay of LTP and the natural active forgetting of LTM (62, 69, 70), which suggests that autophagy plays a role in the forgetting of consolidated memories through the gradual synaptic loss of AMPAR overtime, and, hence, memory loss.

D-cycloserine, an NMDAR agonist, prepares resistant memories for destabilization (71). Noteworthy, d-cycloserine also enhances memory update (fear extinction) by increasing GluA2-containing AMPAR endocytosis, and augments NMDAR-2B-dependent hippocampal LTD (72, 73). Therefore, autophagy might be a potential downstream mechanism by which d-cycloserine facilitates destabilization. We showed here that autophagy destabilizes resistant memories formed under stressful conditions (Figure 3), suggesting autophagy as a potential target for clinical applications. Owing to the growing interest in finding autophagy inducers for several applications, many FDA-approved autophagy inducers already exist, including known anti-psychotic and anti-depressant drugs, and more specific ones are on their way (74, 75). This increases the feasibility of using autophagy inducers for future therapeutic applications, including PTSD treatment.

Recent study demonstrated that engram cells retain the memory after anisomycin-induced partial amnesia, suggesting that synaptic plasticity is dispensable for memory storage (43). However, we proved here that synaptic plasticity between engram assemblies is indispensable for memory storage and that engram network no longer retains the memory after complete amnesia. Our findings are consistent with a recent study showing that LTP isn't induced globally after single fear memory formation (76), nevertheless, they didn't examine whether altering an engram-specific plasticity would have comprehensive effects on other engrams stored in the same ensemble and whether synaptic plasticity is essential for information storage.

Brain machinery that stores and distinguishes between several memories encoded in the same neurons is critically important for organizing the uniqueness of memories. Our study uncovers the mechanism by which brain can maintain the storage and the uniqueness of a massive number of associated memories stored in shared cell ensemble. Furthermore, we show selective and total erasure of fear memory from engram network without affecting other memories stored in the same ensemble by resetting the plasticity in synapse specific manner, leading to better understanding of the mechanism of memory storage and giving more insight into therapeutic ways to treat post-traumatic stress disorder (PTSD).

METHODS

Animals

Naive male C57BL/6J (purchased from Japan SLC, inc) and c-Fos::tTA transgenic mice (Mutant Mouse Regional Resource Center, stock number: 031756-MU) were obtained as described previously (32, 35). The founders of the R26R::H2B-mCherry transgenic mice (CDB0204K) were described previously (77). The progeny for the c-Fos::tTA and cFos::tTA/R26R::H2B-mCherry double-transgenic mouse line were generated using in vitro fertilization with eggs from C57BL/6J mice and embryo transfer techniques. These transgenic mice were raised on food containing 40 mg kg−1 Dox and maintained on Dox pellets except for 2 days before the conditioning session. All mice were maintained on a 12 h light/dark cycle at 24 ± 3°C and 55 ± 5% humidity, had access to food and water ad libitum and housed with littermates until surgery. Mice for behavioral analyses were 12–18 weeks old. All procedures involving the use of animals were performed in accordance with the guidelines of the National Institutes of Health (NIH) and were approved by the Animal Care and Use Committee of the University of Toyama and the Institutional Committee for the Care and Use of Experimental Animals of Jikei University.

Drugs and peptides

Anisomycin (Sigma Aldrich Japan Co., Tokyo, Japan) was dissolved in a minimum quantity of HCl, diluted with phosphate buffered saline (PBS), and adjusted to pH 7.4 with NaOH. Ifenprodil tartrate (Sigma Aldrich Co., Japan) and trifluoperazine dihydrochloride (Sigma Aldrich Japan Co.) were dissolved in PBS. Spautin-1 (Sigma Aldrich Co., Japan) was dissolved in DMSO and diluted with equal volume of saline. The retro-inverso Tat-beclin 1 peptide D-amino acid sequence (RRRQRRKKRGYGGTGFEGDHWIEFTANFVNT; synthesized by

GenScript through Funakoshi Co., Ltd., Tokyo, Japan) was dissolved in either PBS (tBC) or anisomycin solution (Ani+tBC). The Tat-GluA2$_{3Y}$ peptide L-amino acid sequence (YGRKKRRQRRRYKEGYNVYG, AnaSpec, Fremont, CA) and its control Tat-GluA2$_{3A}$ peptide L-amino acid sequence (YGRKKRRQRRRAKEGANVAG; AnaSpec), were both dissolved in PBS (GluA2$_{3Y}$ or GluA2$_{3A}$, respectively). All peptides were aliquoted into single experiment volumes and stored at −80°C.

Viral constructs.

The recombinant AAV vectors used were AAV-TRE$_{3G}$-Cre and AAV-hSyn1-DIO-oChIEF-Citrine at 1:10 ratio. pAAV-hSyn1-DIO-oChIEF-Citrine plasmid was acquired from Addgene (Addgene plasmid 50973). For pAAV-TRE$_{3G}$-Cre preparation, we constructed pAAV-TRE$_{3G}$-CreER^{T2} firstly by replacing the PCR-amplified TRE$_{3G}$-CreER^{T2} of pLenti-TRE$_{3G}$-CreER^{T2} which was described previously (34), with primers (sense, GCGACGCGTCGAATTCGTCTTCAAGAATTCCTC; antisense, CAGGCCGCGGGAAGGAAG) into pAAV-EF1a-DIO-EYFP (donated by Dr. K. Deisseroth) at the *Mlu*I-*Sac*II restriction sites. Then, inverse PCR was performed using pAAV-TRE$_{3G}$-CreER^{T2} template with primers (sense, GGATCATCCATCCATCACAGTGGC; antisense, TTAATCGCCATCTTCCAGCAGGCG) to construct pAAV-TRE$_{3G}$-Cre. The recombinant AAV vectors were produced as described previously (78), and injected with viral titres of 2.8 x 10^{13} vg/mL for AAV9-hSyn1-DIO-oChIEF-Citrine and 1.4 x 10^{13} vg/mL for AAV9-TRE$_{3G}$-Cre.

Stereotactic surgery and drug infusion in mice

Mice were 8–10 weeks old at the time of surgery. They were anesthetized with isoflurane, given an intraperitoneal injection of pentobarbital solution (80 mg/kg of body weight), and then placed in a stereotactic apparatus (Narishige, Tokyo, Japan). Mice were then bilaterally implanted with a stainless guide cannula (PlasticsOne, Roanoke, VA, USA). For targeting the BLA, the guide cannula was positioned 1.5 mm posterior, 3.3 mm lateral, and 3.4 mm ventral to the bregma. For targeting the LA, the guide cannula was positioned 1.7 mm posterior, 3.4 mm lateral, and 2.6 mm ventral to the bregma. After surgery, a cap or dummy cannula (PlasticsOne) was inserted into the guide cannula, and mice were allowed to recover for at least 7 days in individual home cages before the experiment. Mice in the NoFS group were not cannulated. All drug infusions were done under isoflurane anesthesia, using an injection cannula with a 0.25 mm internal diameter (PlasticsOne), and extending beyond the end of the guide cannula by 1.5 mm for the BLA and LA. The drug infusion rate was 0.2 µl/minute for the BLA and LA. Following drug infusion, the injection cannula was left in place for 2 minutes to allow for drug diffusion. In all of these reconsolidation experiments, 1 µl of drug solution contained either PBS, 125 µg of anisomycin, 20 µg of tBC, or 125 µg anisomycin + 20 µg tBC. For autophagy inhibition, 0.5 µl of solution containing 8.3 µg Spautin-1 or vehicle was injected into LA. For blocking AMPA receptor endocytosis, 0.5 µl of solution containing 20 ng of $GluA2_{3Y}$ or $GluA2_{3A}$ was injected into the LA.

For optogenetic experiments, 500 nl of virus were injected at 100 nl min^{-1} bilaterally to the AC (-2.7 mm anteroposterior (AP), ±4.4 mm mediolateral (ML), +3.3 mm dorsoventral (DV)), MGm (-3.1 mm AP, ±1.9 mm ML, +3.5 mm DV) and LA (-1.7 mm AP, ±3.4 mm ML, +4.1 mm DV). After injection, the injection cannula was kept for 5 min before its withdrawal, then a stainless guide cannula (PlasticsOne, Roanoke, VA, USA) targeting LA was positioned 3.1 mm ventral to the bregma and fixed on the skull with dental cement. Then, a dummy cannula

(PlasticsOne) with cap was inserted into the guide cannula. Mice were allowed to recover for at least 7 days in individual home cages before starting the experiments.

Lysate preparation and immunoblot analysis

Drugs were infused into amygdala of one hemisphere of the C57BL/6J mice, as described above. Four hours later, their brains were removed and cut into 1-mm slices, placed on ice, and the amygdala from each hemisphere was dissected under a binocular microscope, rapidly frozen on dry ice, and stored at −80°C. Samples were then sonicated in RIPA buffer (50 mM TrisHCl, pH 7.5, 150 mM NaCl, 2 mM EDTA, 1% NP-40, 0.5% sodium deoxycholate, 0.1% SDS, and 50 mM NaF) containing a protease inhibitor mixture (cOmplete ULTRA tablets, Roche Diagnostics GMBH, Mannheim, Germany) and a phosphatase inhibitor mixture (PhosSTOP tablets, Roche Diagnostics GMBH). Samples were then centrifuged at 14000 rpm for 15 minutes at 4°C, and supernatants were stored at −30°C until use. Measurement of protein concentration, immunoblotting for LC3 detection (ab48394; Abcam, Tokyo, Japan), visualization and quantitation were performed as previously described (3).

Contextual fear conditioning (CFC)

All behavioral sessions were conducted during the light cycle, in a dedicated soundproof behavioral room (Yamaha Co., Shizuoka, Japan), described here as Room A. The CS context was a square chamber (Chamber A) with a plexiglass front, off-white side- and back-walls (length 175 × width 165 × height 300 mm), and a floor consisting of stainless steel rods connected to an electric shock generator. The distinct context was a circular chamber (Chamber B) with opaque reddish walls (diameter 235 mm × height 225 mm), and a smooth gray floor. The light in Room A was adjusted to give ~325 lx in the center of Chamber A and ~850 lx in

the center of Chamber B. After recovery from surgery, a maximum of six mice were moved from their home cages on racks in the maintenance room (~ 260 ± 70 lx), to the experimental room equipped with a covered stainless-steel waiting rack (~60 ± 13 lx). One day before the experiment, mice were left undisturbed in the waiting rack for 2 h for habituation purposes. On the day of the experiment, mice were left undisturbed in the waiting rack for at least 30 minutes before and after each session, and during the experiment. In each session, one mouse in its home cage was moved into Room A. During the conditioning or reconditioning sessions, mice were placed in Chamber A and allowed to explore for 148 sec, before receiving one footshock (2 sec, 0.4 mA). They then remained for 30 sec, before being moved back to their home cages and returned to the waiting rack. During the retrieval session (T1), mice were placed back into Chamber A for 3 minutes, then immediately subjected to isoflurane anesthesia and drug infusion. Mice in the NoFS group were manipulated identically, with the exceptions that the shock generator was turned off and they were not subjected to anesthesia. During the test sessions, mice were placed back into Chamber A (T2 and T4) for 5 minutes, and 1 h later into Chamber B (T3) for 5 minutes. Mice remained in the waiting rack during the 1 h interval. In all behavioral sessions, chambers were cleaned with 70% ethanol and water between each mouse, and kept odorless to the experimenter.

Auditory fear conditioning

Different chambers were used for each auditory fear conditioning session. Context exploration and conditioning were performed in Chamber A, using the same light adjustment as in the CFC. Retrieval sessions were performed in a circular chamber (Chamber C) with opaque black walls (diameter 215 mm × height 340 mm) and a smooth gray floor. Test sessions were performed in a circular chamber (Chamber D) with opaque reddish walls (diameter 235 mm × height 310

mm) and a smooth gray floor. The light in Room A was adjusted to give ~325 lx in the center of Chamber A, ~820 lx in the center of Chamber C, and ~300 lx in the center of Chamber D. After recovery from surgery, a maximum of six mice were moved from their home cages on racks in the maintenance room to a soundproof (Yamaha Co.) waiting room (Room B). Mice were left undisturbed for at least 15 minutes before and after each session, and during the experiment. In each session, one mouse in its home cage was moved into Room A. During the context exploration sessions, mice were placed in Chamber A and allowed to explore for 5 minutes per day for 2 days. During the conditioning sessions, mice were placed in Chamber A for 2 minutes, and then received one or three tones (30 sec, 65 dB, 7 kHz), co-terminating with a shock (2 sec, 0.4 mA), with an interval of 30 sec. After the last shock, mice remained for 30 sec, and were then returned to their home cages and to Room B. During the retrieval sessions, mice were placed into Chamber C for 2 minutes before receiving a tone (30 sec, 65 dB, 7 kHz), then 30 sec later, mice were subjected to isoflurane anesthesia and drug infusion before being returned to Room B. For autophagy inhibition or blocking of AMPA receptor endocytosis, mice were subjected to isoflurane anesthesia and drug infusion 75 minutes prior to the retrieval sessions. During test sessions, mice were placed in Chamber D for 2 minutes, and then received a tone (30 sec, 65 dB, 7 kHz).

Auditory fear conditioning with optogenetic manipulation. Different chambers were used for each auditory fear conditioning session. All chambers were different in shape, lightening pattern and texture of the floor. The experiments were performed on AAV-injected c-fos-tTA mice, maintained on food containing 40 mg/kg doxycycline.

Habituation. Three-four weeks after virus infection, mice were allowed to explore the context for 2 minutes before exposing them to a neutral tone (30 sec, 65 dB, 2 kHz), mice remained for additional 2.5 minutes before returning to their home cages. After the second habituation session, doxycycline was removed and mice were maintained on normal food.

Conditioning. Two days later, mice were placed in the context for 2 minutes, and then received single presentation of a conditioned tone (30 sec, 65 dB, 7 kHz), co-terminating with a shock (2 sec, 0.4 mA), mice remained for 30 sec, and were then returned to their home cages. Six hours later, the food was changed to one containing 1000 mg/kg doxycycline.

Testing. Mice were allowed to explore unfamiliar context for 2 minutes before receiving the tested tone (30 sec, 65 dB, 7 kHz or 2kHz), then 30 sec later, mice were returned to their home cages except for Test 1 only, they were subjected to isoflurane anesthesia and drug infusion.

Optogenetic stimulation (10 & 20 Hz). For the placement of two branch-typed optical fibers (internal diameter, 0.25 mm) connected to a housing with a cap, mice were anaesthetized with approximately 2.0% isoflurane and the optic fibers were inserted into guide cannulas. The tip of the optical fiber was targeted 0.5 mm above LA (DV 3.6 mm from bregma). Mice with the inserted optic fibers were then returned to their home cages and left for at least for 2 h. The fiber unit-connected mouse was attached to an optical swivel, which was connected to a laser unit (8–10 mW, 473 nm). The delivery of light was controlled using a schedule stimulator in time-lapse Mode. Optogenetic session was 9 minutes in duration consisting of three 3 min epochs with the first and third epochs were Light-Off epochs while the second one was Light-On epoch. During Light-On epoch mice received optical stimulation (10 Hz or 20 Hz, 15 ms pulse width) for the entire 3 min. One hour after the end of the session, the fiber was removed from the cannula under anesthesia.

In vivo LTP induction. Immediately after Test 4, mice were placed in different home cage and after 2 minutes exploration, optical LTP was induced with 10 trains of light (each train consisted of 100 pulses of light, 5 ms each, at 100 Hz) at 90-s inter-train intervals.

Experiments consisting of two overlapping memories (Figure 11, 12)

Habituation, testing and optogenetic stimulation sessions were described above.

Conditioning**.** After two days off DOX, mice were fear conditioned to 7kHz tone as described above. Immediately after the session, mice were put back on food containing 1000 mg/kg doxycycline. One hour later, mice were injected intraperitoneal with doxycycline hyclate (120 mg / kg) to stop the expression of oChIEF. Five hours or 24 hours after 7kHz fear conditioning, mice were exposed to 2kHz fear conditioning.

In vivo LTP or LTD induction. Immediately after test session, optical LTP or LTD was applied. Optical LTP was induced with 10 trains of light (each train consisted of 100 pulses of light, 5 ms each, at 100 Hz) at 90-s inter-train intervals. Optical LTD was induced with 900 pulses of light, 2 ms each, at 1 Hz.

Two tones discrimination experiment (Figure 5)

Naive male C57BL/6J mice were used. Mice were exposed to the above-mentioned protocol during the habituation and conditioning sessions. One day after conditioning, mice were divided into two groups, the first one was tested with 7kHz tone first, then tested with 2kHz tone on the next day, while the second group was tested with 2kHz tone first, then tested with 7kHz tone. During test session, mice allowed to explore unfamiliar context for 2 minutes before receiving the tested tone then 30 sec later, mice were returned to their home cages.

Behavioral analysis

All experiments were conducted using a video tracking system (Muromachi Kikai, Tokyo, Japan) to measure the freezing behavior of the animals. Freezing was defined as a complete absence of movement, except for respiration. We started scoring the duration of the FR after 1 sec of sustained freezing behavior. All behavioral sessions were screen recorded using Bandicam software (Bandisoft, Seoul, Korea). Occupancy plots representing the maximum occupancy of the mouse center in the defined context space during each session were generated by analyzing the screen recorded movies using ANY-maze software (Stoelting Co., Wood Dale,

IL, USA). Mice were assessed as completely amnesic when they: (1) showed at least a 50% decrease in freezing level after drug infusion compared with the level before treatment, and (2) showed a freezing level in the CS or distinct contexts within the 95% confidence interval of the freezing level of the NoFS group (used as a reference for normal mouse behavior). Animals were excluded from behavioral analysis when showing abnormal behavior after surgery or the cannula was misplaced in position.

In vivo LTP or LTD induction.

For behavior experiments, optical LTP was induced with 10 trains of light (each train consisted of 100 pulses of light, 5 ms each, at 100 Hz) at 90-s inter-train intervals. Optical LTD was induced with 900 pulses of light, 2 ms each, at 1 Hz.

For LTP occlusion experiment, optical LTP was induced with 5 trains of light (each train consisted of 100 pulses of light, 5 ms each, at 100 Hz) at 3 minutes inter-train intervals.

***In vivo* recording.**

Four weeks after the injection of AAV viral vectors into the MGm and AC, mice were anesthetized with pentobarbital and then mounted on a stereotaxic frame. The optic fiber was glued to the recording tungsten electrode so that the tip of the fiber was 500 μm above the tip of the electrode. The optrode was inserted into the LA and the optic fiber was connected to a 473-nm laser unit. The LTP or LTD induction protocol was identical to that used in the behavioral test. After establishing a stable baseline at the recording site for 20 min (stimulation frequency at 0.033 Hz), in vivo LTP or LTD was optically induced, which was followed by at least 20 min of 0.033 Hz stimulation. Data were analyzed using Clampex 10.7 software. All animals were perfused after the recordings and the position of the recording sites were verified.

LTP occlusion experiment.

Behavior was done as described above. One day after test session and drug infusion, mice were anesthetized and the guide cannulas with the dental cement were removed from the skull. Then we performed *in vivo* recording as described above.

Immunohistochemistry

One and half hour after the desired session, the mice were deeply anesthetized with pentobarbital solution, and perfused transcardially with PBS (pH 7.4) followed by 4% paraformaldehyde in PBS (PFA). The brains were removed, further post-fixed by immersion in PFA for 12–18 h at 4°C, equilibrated in 25% sucrose in PBS for 36–48 h at 4°C, and then stored at –80°C. Brains were cut into 50 μm coronal sections using a cryostat and transferred to 12-well cell culture plates (Corning, NY, USA) containing PBS. After washing with PBS, the floating sections were treated with blocking buffer (3% normal donkey serum; S30, Chemicon by EMD Millipore, Billerica, MA USA) in PBS containing 0.2% Triton X-100 and 0.05% tween 20 (PBST) at room temperature (RT) for 1 h. The following primary antibodies were applied in blocking buffer at 4°C for 24-36 h: rat anti-GFP (1:1000, Nacalai Tesque, 04404-84, GF090R), rabbit anti-c-Fos (1:1000, Santa Cruz Biotechnology, sc-7202), goat anti-c-Fos (1:1000, Santa Cruz Biotechnology, sc-52-G) and rabbit anti-mCherry (1:1000, Clontech, 632496). After three 10-minute washes with 0.2% PBST, sections were incubated in blocking buffer at RT for 2–3 h with the following corresponding secondary antibodies: donkey anti-rat IgG Alexa Fluor 488 (1:1000, Molecular Probes, A21208) or donkey anti-rabbit IgG Alexa Fluor 546 (1:1000, Molecular Probes, A10040) or donkey anti-goat IgG Alexa Fluor 647 (1:1000, Molecular Probes, A21447). Finally, the sections were treated with DAPI (1 μg/ml,

Roche Diagnostics, 10236276001) and then washed with 0.2% PBST three times for 10 min each before being mounted onto slide glass with ProLong Gold antifade reagent (Invitrogen).

Confocal microscopy and cell counting.

Images were acquired using a Zeiss LSM 780 confocal microscope (Carl Zeiss, Jena, Germany) with plan apochromat lens using 20× objective. All acquisition parameters were kept constant within each magnification. To quantify the number of each immunoreactive cell in target regions after collecting z-stacks (approximately ten optical sections of 10 μm thick), three coronal sections per mouse (n = 4 mice) were manually counted. Overlaps between the GFP+ and c-fos+ cells as well as mCherry+ and c-fos+ cells were manually counted.

Statistics

Statistical analysis was performed using Prism 6.01 or InStat 3.1 (GraphPad Software, San Diego, CA, USA). Data from two groups were compared using two-tailed unpaired Student t tests. Multiple-group comparisons were assessed using ANOVA with post hoc tests. Quantitative data are presented as mean ± s.e.m.

REFERENCES

1. Tronson NC, Taylor JR. Molecular mechanisms of memory reconsolidation. Nat Rev Neurosci. 2007;8(4):262-75.

2. Quirk GJ, Mueller D. Neural mechanisms of extinction learning and retrieval. Neuropsychopharmacology. 2008;33(1):56-72.

3. Davis HP, Squire LR. Protein synthesis and memory: a review. Psychol Bull. 1984;96(3):518-59.

4. Nader K, Schafe GE, Le Doux JE. Fear memories require protein synthesis in the amygdala for reconsolidation after retrieval. Nature. 2000;406(6797):722-6.

5. Lee SH, Choi JH, Lee N, Lee HR, Kim JI, Yu NK, et al. Synaptic protein degradation underlies destabilization of retrieved fear memory. Science. 2008;319(5867):1253-6.

6. Besnard A, Caboche J, Laroche S. Reconsolidation of memory: a decade of debate. Prog Neurobiol. 2012;99(1):61-80.

7. Finnie PS, Nader K. The role of metaplasticity mechanisms in regulating memory destabilization and reconsolidation. Neurosci Biobehav Rev. 2012;36(7):1667-707.

8. Lee JLC, Nader K, Schiller D. An Update on Memory Reconsolidation Updating. Trends in Cognitive Sciences. 2017.

9. Inaba H, Tsukagoshi A, Kida S. PARP-1 activity is required for the reconsolidation and extinction of contextual fear memory. Mol Brain. 2015;8(1):63.

10. Pitman RK. Will reconsolidation blockade offer a novel treatment for posttraumatic stress disorder? Front Behav Neurosci. 2011;5:11.

11. Mizushima N, Komatsu M. Autophagy: renovation of cells and tissues. Cell. 2011;147(4):728-41.

12. Yamamoto A, Yue Z. Autophagy and its normal and pathogenic states in the brain. Annu Rev Neurosci. 2014;37:55-78.

13. Ohsumi Y. Historical landmarks of autophagy research. Cell Res. 2014;24(1):9-23.

14. Mizushima N, Yoshimori T, Ohsumi Y. The role of Atg proteins in autophagosome formation. Annu Rev Cell Dev Biol. 2011;27:107-32.

15. Hara T, Nakamura K, Matsui M, Yamamoto A, Nakahara Y, Suzuki-Migishima R, et al. Suppression of basal autophagy in neural cells causes neurodegenerative disease in mice. Nature. 2006;441(7095):885-9.

16. Komatsu M, Waguri S, Chiba T, Murata S, Iwata J, Tanida I, et al. Loss of autophagy in the central nervous system causes neurodegeneration in mice. Nature. 2006;441(7095):880-4.

17. Liang CC, Wang C, Peng X, Gan B, Guan JL. Neural-specific deletion of FIP200 leads to cerebellar degeneration caused by increased neuronal death and axon degeneration. J Biol Chem. 2010;285(5):3499-509.

18. Shehata M, Inokuchi K. Does autophagy work in synaptic plasticity and memory? Rev Neurosci. 2014;25(4):543-57.

19. Bingol B, Sheng M. Deconstruction for reconstruction: the role of proteolysis in neural plasticity and disease. Neuron. 2011;69(1):22-32.

20. Hollenbeck PJ. Products of endocytosis and autophagy are retrieved from axons by regulated retrograde organelle transport. J Cell Biol. 1993;121(2):305-15.

21. Shehata M, Matsumura H, Okubo-Suzuki R, Ohkawa N, Inokuchi K. Neuronal stimulation induces autophagy in hippocampal neurons that is involved in AMPA receptor degradation after chemical long-term depression. J Neurosci. 2012;32(30):10413-22.

22. Rowland AM, Richmond JE, Olsen JG, Hall DH, Bamber BA. Presynaptic terminals independently regulate synaptic clustering and autophagy of GABAA receptors in Caenorhabditis elegans. J Neurosci. 2006;26(6):1711-20.

23. Nabavi S, Fox R, Proulx CD, Lin JY, Tsien RY, Malinow R. Engineering a memory with LTD and LTP. Nature. 2014;511(7509):348-52.

24. Kessels HW, Malinow R. Synaptic AMPA receptor plasticity and behavior. Neuron. 2009;61(3):340-50.

25. Squire LR, Kandel ER. Memory : from mind to molecules. 2nd ed. Greenwood Village, Colo.: Roberts & Co.; 2009. xi, 256 p. p.

26. Chen X, Garelick MG, Wang H, Lil V, Athos J, Storm DR. PI3 kinase signaling is required for retrieval and extinction of contextual memory. Nat Neurosci. 2005;8(7):925-31.

27. Gafford GM, Parsons RG, Helmstetter FJ. Consolidation and reconsolidation of contextual fear memory requires mammalian target of rapamycin-dependent translation in the dorsal hippocampus. Neuroscience. 2011;182:98-104.

28. Josselyn SA, Kohler S, Frankland PW. Finding the engram. Nat Rev Neurosci. 2015;16(9):521-34.

29. Tonegawa S, Liu X, Ramirez S, Redondo R. Memory Engram Cells Have Come of Age. Neuron. 2015;87(5):918-31.

30. Cai DJ, Aharoni D, Shuman T, Shobe J, Biane J, Song W, et al. A shared neural ensemble links distinct contextual memories encoded close in time. Nature. 2016;534(7605):115-8.

31. Nomoto M, Ohkawa N, Nishizono H, Yokose J, Suzuki A, Matsuo M, et al. Cellular tagging as a neural network mechanism for behavioural tagging. Nat Commun. 2016;7:12319.

32. Ohkawa N, Saitoh Y, Suzuki A, Tsujimura S, Murayama E, Kosugi S, et al. Artificial association of pre-stored information to generate a qualitatively new memory. Cell Rep. 2015;11(2):261-9.

33. Rashid AJ, Yan C, Mercaldo V, Hsiang HL, Park S, Cole CJ, et al. Competition between engrams influences fear memory formation and recall. Science. 2016;353(6297):383-7.

34. Yokose J, Okubo-Suzuki R, Nomoto M, Ohkawa N, Nishizono H, Suzuki A, et al. Overlapping memory trace indispensable for linking, but not recalling, individual memories. Science. 2017;355(6323):398-403.

35. Reijmers LG, Perkins BL, Matsuo N, Mayford M. Localization of a stable neural correlate of associative memory. Science. 2007;317(5842):1230-3.

36. Rogerson T, Cai DJ, Frank A, Sano Y, Shobe J, Lopez-Aranda MF, et al. Synaptic tagging during memory allocation. Nat Rev Neurosci. 2014;15(3):157-69.

37. Bliss TV, Lomo T. Long-lasting potentiation of synaptic transmission in the dentate area of the anaesthetized rabbit following stimulation of the perforant path. J Physiol. 1973;232(2):331-56.

38. Bocchio M, Nabavi S, Capogna M. Synaptic Plasticity, Engrams, and Network Oscillations in Amygdala Circuits for Storage and Retrieval of Emotional Memories. Neuron. 2017;94(4):731-43.

39. Citri A, Malenka RC. Synaptic plasticity: multiple forms, functions, and mechanisms. Neuropsychopharmacology. 2008;33(1):18-41.

40. Neves G, Cooke SF, Bliss TV. Synaptic plasticity, memory and the hippocampus: a neural network approach to causality. Nat Rev Neurosci. 2008;9(1):65-75.

41. Johansen JP, Cain CK, Ostroff LE, LeDoux JE. Molecular mechanisms of fear learning and memory. Cell. 2011;147(3):509-24.

42. Roy DS, Arons A, Mitchell TI, Pignatelli M, Ryan TJ, Tonegawa S. Memory retrieval by activating engram cells in mouse models of early Alzheimer's disease. Nature. 2016;531(7595):508-12.

43. Ryan TJ, Roy DS, Pignatelli M, Arons A, Tonegawa S. Memory. Engram cells retain memory under retrograde amnesia. Science. 2015;348(6238):1007-13.

44. Tonegawa S, Pignatelli M, Roy DS, Ryan TJ. Memory engram storage and retrieval. Curr Opin Neurobiol. 2015;35:101-9.

45. Marsh T, Debnath J. Ironing out VPS34 inhibition. Nat Cell Biol. 2015;17(1):1-3.

46. De Leo MG, Staiano L, Vicinanza M, Luciani A, Carissimo A, Mutarelli M, et al. Autophagosome-lysosome fusion triggers a lysosomal response mediated by TLR9 and controlled by OCRL. Nat Cell Biol. 2016;18(8):839-50.

47. Shoji-Kawata S, Sumpter R, Leveno M, Campbell GR, Zou Z, Kinch L, et al. Identification of a candidate therapeutic autophagy-inducing peptide. Nature. 2013;494(7436):201-6.

48. Vanhaesebroeck B, Guillermet-Guibert J, Graupera M, Bilanges B. The emerging mechanisms of isoform-specific PI3K signalling. Nat Rev Mol Cell Biol. 2010;11(5):329-41.

49. Liu J, Xia H, Kim M, Xu L, Li Y, Zhang L, et al. Beclin1 controls the levels of p53 by regulating the deubiquitination activity of USP10 and USP13. Cell. 2011;147(1):223-34.

50. Suzuki A, Josselyn SA, Frankland PW, Masushige S, Silva AJ, Kida S. Memory reconsolidation and extinction have distinct temporal and biochemical signatures. J Neurosci. 2004;24:4787-95.

51. Mamiya N, Fukushima H, Suzuki A, Matsuyama Z, Homma S, Frankland PW, et al. Brain region-specific gene expression activation required for reconsolidation and extinction of contextual fear memory. J Neurosci. 2009;29:402-13.

52. Rao-Ruiz P, Rotaru DC, van der Loo RJ, Mansvelder HD, Stiedl O, Smit AB, et al. Retrieval-specific endocytosis of GluA2-AMPARs underlies adaptive reconsolidation of contextual fear. Nat Neurosci. 2011;14(10):1302-8.

53. Kim CH, Chung HJ, Lee HK, Huganir RL. Interaction of the AMPA receptor subunit GluR2/3 with PDZ domains regulates hippocampal long-term depression. Proc Natl Acad Sci U S A. 2001;98(20):11725-30.

54. Scholz R, Berberich S, Rathgeber L, Kolleker A, Kohr G, Kornau HC. AMPA receptor signaling through BRAG2 and Arf6 critical for long-term synaptic depression. Neuron. 2010;66(5):768-80.

55. Lee SH, Liu L, Wang YT, Sheng M. Clathrin adaptor AP2 and NSF interact with overlapping sites of GluR2 and play distinct roles in AMPA receptor trafficking and hippocampal LTD. Neuron. 2002;36(4):661-74.

56. Ahmadian G, Ju W, Liu L, Wyszynski M, Lee SH, Dunah AW, et al. Tyrosine phosphorylation of GluR2 is required for insulin-stimulated AMPA receptor endocytosis and LTD. EMBO J. 2004;23(5):1040-50.

57. Fanselow MS. Contextual fear, gestalt memories, and the hippocampus. Behav Brain Res. 2000;110(1-2):73-81.

58. Huang CC, Chen CC, Liang YC, Hsu KS. Long-term potentiation at excitatory synaptic inputs to the intercalated cell masses of the amygdala. Int J Neuropsychopharmacol. 2014;17(8):1233-42.

59. Park S, Lee J, Park K, Kim J, Song B, Hong I, et al. Sound tuning of amygdala plasticity in auditory fear conditioning. Sci Rep. 2016;6:31069.

60. Tsvetkov E, Carlezon WA, Benes FM, Kandel ER, Bolshakov VY. Fear conditioning occludes LTP-induced presynaptic enhancement of synaptic transmission in the cortical pathway to the lateral amygdala. Neuron. 2002;34(2):289-300.

61. Wenthold RJ, Petralia RS, Blahos J, II, Niedzielski AS. Evidence for multiple AMPA receptor complexes in hippocampal CA1/CA2 neurons. J Neurosci. 1996;16(6):1982-9.

62. Dong Z, Han H, Li H, Bai Y, Wang W, Tu M, et al. Long-term potentiation decay and memory loss are mediated by AMPAR endocytosis. J Clin Invest. 2015;125(1):234-47.

63. Migues PV, Hardt O, Wu DC, Gamache K, Sacktor TC, Wang YT, et al. PKMzeta maintains memories by regulating GluR2-dependent AMPA receptor trafficking. Nat Neurosci. 2010;13(5):630-4.

64. Migues PV, Hardt O, Finnie P, Wang YW, Nader K. The maintenance of long-term memory in the hippocampus depends on the interaction between N-ethylmaleimide-sensitive factor and GluA2. Hippocampus. 2014;24(9):1112-9.

65. Yao Y, Kelly MT, Sajikumar S, Serrano P, Tian D, Bergold PJ, et al. PKM zeta maintains late long-term potentiation by N-ethylmaleimide-sensitive factor/GluR2-dependent trafficking of postsynaptic AMPA receptors. J Neurosci. 2008;28(31):7820-7.

66. Brebner K, Wong TP, Liu L, Liu Y, Campsall P, Gray S, et al. Nucleus accumbens long-term depression and the expression of behavioral sensitization. Science. 2005;310(5752):1340-3.

67. Dalton GL, Wang YT, Floresco SB, Phillips AG. Disruption of AMPA receptor endocytosis impairs the extinction, but not acquisition of learned fear. Neuropsychopharmacology. 2008;33(10):2416-26.

68. Hong I, Kim J, Kim J, Lee S, Ko HG, Nader K, et al. AMPA receptor exchange underlies transient memory destabilization on retrieval. Proc Natl Acad Sci U S A. 2013;110(20):8218-23.

69. Hardt O, Nader K, Wang YT. GluA2-dependent AMPA receptor endocytosis and the decay of early and late long-term potentiation: possible mechanisms for forgetting of short- and long-term memories. Philos Trans R Soc Lond B Biol Sci. 2014;369(1633):20130141.

70. Migues PV, Liu L, Archbold GE, Einarsson EO, Wong J, Bonasia K, et al. Blocking Synaptic Removal of GluA2-Containing AMPA Receptors Prevents the Natural Forgetting of Long-Term Memories. J Neurosci. 2016;36(12):3481-94.

71. Bustos SG, Giachero M, Maldonado H, Molina VA. Previous stress attenuates the susceptibility to Midazolam's disruptive effect on fear memory reconsolidation: influence of pre-reactivation D-cycloserine administration. Neuropsychopharmacology. 2010;35(5):1097-108.

72. Bai Y, Zhou L, Wu X, Dong Z. D-serine enhances fear extinction by increasing GluA2-containing AMPA receptor endocytosis. Behav Brain Res. 2014;270:223-7.

73. Duffy S, Labrie V, Roder JC. D-serine augments NMDA-NR2B receptor-dependent hippocampal long-term depression and spatial reversal learning. Neuropsychopharmacology. 2008;33(5):1004-18.

74. Levine B, Packer M, Codogno P. Development of autophagy inducers in clinical medicine. J Clin Invest. 2015;125(1):14-24.

75. Morel E, Mehrpour M, Botti J, Dupont N, Hamai A, Nascimbeni AC, et al. Autophagy: A Druggable Process. Annu Rev Pharmacol Toxicol. 2017;57:375-98.

76. Kim WB, Cho J-H. Encoding of Discriminative Fear Memory by Input-Specific LTP in the Amygdala. Neuron. 2017;95:1-18.

77. Abe T, Kiyonari H, Shioi G, Inoue K, Nakao K, Aizawa S, Fujimori T. Establishment of conditional reporter mouse lines at ROSA26 locus for live cell imaging. Genesis. 2011;49:579– 90.

78. Iida, A, Takino N, Miyauchi H, Shimazaki K, Muramatsu S. Systemic delivery of tyrosine-mutant AAV vectors results in robust transduction of neurons in adult mice. Bio Med Res Int. 2013;974819.